

University of Tennessee at Chattanooga

UTC Scholar

---

Honors Theses

Student Research, Creative Works, and  
Publications

---

5-2020

## Melamine-derived graphene foam as a thermal additive for water harvesting applications

Emily Chase

University of Tennessee at Chattanooga, [jj444@mocs.utc.edu](mailto:jj444@mocs.utc.edu)

Follow this and additional works at: <https://scholar.utc.edu/honors-theses>



Part of the [Hydraulic Engineering Commons](#)

---

### Recommended Citation

Chase, Emily, "Melamine-derived graphene foam as a thermal additive for water harvesting applications" (2020). *Honors Theses*.

This Theses is brought to you for free and open access by the Student Research, Creative Works, and Publications at UTC Scholar. It has been accepted for inclusion in Honors Theses by an authorized administrator of UTC Scholar. For more information, please contact [scholar@utc.edu](mailto:scholar@utc.edu).

# **Melamine-Derived Graphene Foam as a Thermal Additive for Water Harvesting Applications**

Emily Katherine Chase

Departmental Honors Thesis

The University of Tennessee at Chattanooga

Department of Civil and Chemical Engineering

Examination Date:

March 27, 2020

Sungwoo Yang, Ph.D.

Assistant Professor of Civil and Chemical  
Engineering

Thesis Director

Soubantika Palchoudhury, Ph.D.

Assistant Professor of Civil and Chemical  
Engineering

Department Examiner

## **Abstract**

This project proposes the use of a novel melamine-derived graphene foam formed by high temperature pyrolysis under inert conditions for use as a thermal additive to absorbent crystals. The high thermal conductivity of graphene foam makes it an ideal candidate for use as a cheap, flexible, and light-weight alternative to previously used copper foam and metal organic frameworks. Following surface functionalization, graphene foam may be saturated with hydrophilic absorbent crystals.

The primary objectives of this research are to optimize the synthesis process of such a graphene foam to obtain the highest purity product while maintaining foam flexibility and to study the foam's material properties after saturation with a zeolite solution. Manipulated parameters in the optimization process include annealing temperature, annealing time, and ramping rate. Product purity is assessed using Raman spectroscopy. Scanning Electron Microscopy (SEM) is used to compare the deformation of the carbon foam before and after compression. It was found that high annealing temperatures yield the least flexible foam. A temperature of 800°C produced the most flexible foam. Annealing time was found to have an insignificant effect on flexibility and the effects of ramping rate were inconclusive.

## Table of Contents

Abstract.....	2
Table of Contents .....	3
Table of Figures.....	5
Table of Tables .....	10
Chapter 1: Scope of Work.....	11
1.1 Initial Focus .....	11
1.2 Shift in Focus .....	11
1.3 Final Focus.....	11
Chapter 2: Introduction .....	12
2.1 Motivation.....	12
2.2 Background .....	12
Chapter 3: Methods and Materials .....	14
3.1 Experimental Setup .....	14
3.2 Pyrolysis Procedure .....	16
3.3 Mechanical Strength Characterization.....	18
3.4 Raman Spectroscopy .....	20
3.5 Addition of Zeolites.....	21
Chapter 4: Results and Discussion .....	22
4.1 Mechanical Strength and Flexibility .....	22
4.1.1 Effect of Annealing Temperature .....	22
4.1.2 Effect of Annealing Time .....	28
4.1.3 Effect of Ramping Rate .....	33
4.2 Raman Spectroscopy and Literature Review.....	36
4.3 Addition of Zeolite .....	38
4.4 Potential Sources of Error.....	40
Chapter 5: Conclusions .....	41
5.1 Conclusion and Recommendations .....	41
5.2 Future Work.....	41
References .....	43
Appendices.....	45
Appendix 1: Safety Measures .....	45
Appendix 2: Project Outcomes .....	45

<b>Appendix 3: Raw Data.....</b>	<b>45</b>
Appendix 3.1: Flexibility Testing- Counts .....	45
Appendix 3.2: Additional SEM Images.....	60

## Table of Figures

Figure 1 Flow meter.....	15
Figure 2 Lindberg/Blue Mini-Mite Tube Furnace and piping setup.....	16
Figure 3 Athena XT16 Temperature/Process Controller .....	16
Figure 4 Graphene foam structure .....	18
Figure 5 Graphene foam structure after compression.....	19
Figure 6 Area selected for analysis.....	20
Figure 7 Breaks per 100 $\mu\text{m}^2$ in graphene foam synthesized at various annealing temperatures. 23	
Figure 8 Ratio of breaks to intact strands per 100 $\mu\text{m}^2$ in graphene foam synthesized at various annealing temperatures .....	24
Figure 9 Graphene foam synthesized at 700°C following compression.....	25
Figure 10 Graphene foam synthesized at 800°C following compression.....	26
Figure 11 Graphene foam synthesized at 900°C following compression.....	26
Figure 12 Graphene foam synthesized at 1000°C following compression.....	27
Figure 13 Breaks per 100 $\mu\text{m}^2$ in graphene foam synthesized at various annealing times.....	28
Figure 14 Ratio of breaks to intact strands per 100 $\mu\text{m}^2$ in graphene foam synthesized at various annealing times .....	29
Figure 15 Graphene foam annealed for 90 minutes then compressed .....	30
Figure 16 Graphene foam annealed for 15 minutes then compressed .....	31
Figure 17 Graphene foam annealed for 30 minutes then compressed .....	31
Figure 18 Graphene foam annealed for 45 minutes then compressed .....	32
Figure 19 Breaks per 100 $\mu\text{m}^2$ in graphene foam synthesized at various ramping rates .....	33
Figure 20 Ratio of breaks to intact strands per 100 $\mu\text{m}^2$ in graphene foam synthesized at various annealing times .....	34
Figure 21 Graphene foam synthesized at a ramping rate of 15°C/min after compression .....	35

Figure 22 Raman spectroscopy of graphene foam synthesized at various annealing temperatures .....	36
Figure 23 Raman spectroscopy of graphene foam synthesized at various annealing times .....	37
Figure 24 Raman spectroscopy of graphene foam synthesized at various ramping rates .....	37
Figure 25 Graphene foam saturated with Z-02 .....	39
Figure 26 Graphene foam saturated with 13X .....	40
Figure 27 SEM image 1 of graphene foam synthesized at 700°C, ramping rate of 10°C/min, and a total reaction time of 140 minutes (annealed for 70 minutes) .....	46
Figure 28 SEM image 2 of graphene foam synthesized at 700°C, ramping rate of 10°C/min, and a total reaction time of 140 minutes (annealed for 70 minutes) .....	46
Figure 29 SEM image 3 of graphene foam synthesized at 700°C, ramping rate of 10°C/min, and a total reaction time of 140 minutes (annealed for 70 minutes) .....	47
Figure 30 SEM image 4 of graphene foam synthesized at 700°C, ramping rate of 10°C/min, and a total reaction time of 140 minutes (annealed for 70 minutes) .....	47
Figure 31 SEM image 1 of graphene foam synthesized at 800°C, ramping rate of 10°C/min, and a total reaction time of 140 minutes (annealed for 60 minutes) .....	48
Figure 32 SEM image 2 of graphene foam synthesized at 800°C, ramping rate of 10°C/min, and a total reaction time of 140 minutes (annealed for 60 minutes) .....	48
Figure 33 SEM image 1 of graphene foam synthesized at 900°C, ramping rate of 10°C/min, and a total reaction time of 140 minutes (annealed for 50 minutes) .....	49
Figure 34 SEM image 1 of graphene foam synthesized at 1000°C, ramping rate of 10°C/min, and a total reaction time of 140 minutes (annealed for 40 minutes) .....	49
Figure 35 SEM image 1 of graphene foam synthesized at 1000°C, ramping rate of 15°C/min, and a total reaction time of 140 minutes (annealed for 73 minutes) .....	50
Figure 36 SEM image 2 of graphene foam synthesized at 1000°C, ramping rate of 15°C/min, and a total reaction time of 140 minutes (annealed for 73 minutes) .....	50
Figure 37 SEM image 3 of graphene foam synthesized at 1000°C, ramping rate of 15°C/min, and a total reaction time of 140 minutes (annealed for 73 minutes) .....	51
Figure 38 SEM image 4 of graphene foam synthesized at 1000°C, ramping rate of 15°C/min, and a total reaction time of 140 minutes (annealed for 73 minutes) .....	51

Figure 39 SEM image 5 of graphene foam synthesized at 1000°C, ramping rate of 15°C/min, and a total reaction time of 140 minutes (annealed for 73 minutes) .....	52
Figure 40 SEM image 1 of graphene foam synthesized at 1000°C, ramping rate of 20°C/min, and a total reaction time of 140 minutes (annealed for 90 minutes) .....	52
Figure 41 SEM image 2 of graphene foam synthesized at 1000°C, ramping rate of 20°C/min, and a total reaction time of 140 minutes (annealed for 90 minutes) .....	53
Figure 42 SEM image 3 of graphene foam synthesized at 1000°C, ramping rate of 20°C/min, and a total reaction time of 140 minutes (annealed for 90 minutes) .....	53
Figure 43 SEM image 4 of graphene foam synthesized at 1000°C, ramping rate of 20°C/min, and a total reaction time of 140 minutes (annealed for 90 minutes) .....	54
Figure 44 SEM image 5 of graphene foam synthesized at 1000°C, ramping rate of 20°C/min, and a total reaction time of 140 minutes (annealed for 90 minutes) .....	54
Figure 45 SEM image 6 of graphene foam synthesized at 1000°C, ramping rate of 20°C/min, and a total reaction time of 140 minutes (annealed for 90 minutes) .....	55
Figure 46 SEM image 1 of graphene foam synthesized at 1000°C, ramping rate of 20°C/min, and a total reaction time of 65 minutes (annealed for 15 minutes) .....	55
Figure 47 SEM image 2 of graphene foam synthesized at 1000°C, ramping rate of 20°C/min, and a total reaction time of 65 minutes (annealed for 15 minutes) .....	56
Figure 48 SEM image 3 of graphene foam synthesized at 1000°C, ramping rate of 20°C/min, and a total reaction time of 65 minutes (annealed for 15 minutes) .....	56
Figure 49 SEM image 4 of graphene foam synthesized at 1000°C, ramping rate of 20°C/min, and a total reaction time of 65 minutes (annealed for 15 minutes) .....	57
Figure 50 SEM image 5 of graphene foam synthesized at 1000°C, ramping rate of 20°C/min, and a total reaction time of 65 minutes (annealed for 15 minutes) .....	57
Figure 51 SEM image 6 of graphene foam synthesized at 1000°C, ramping rate of 20°C/min, and a total reaction time of 65 minutes (annealed for 15 minutes) .....	58
Figure 52 SEM image 1 of graphene foam synthesized at 1000°C, ramping rate of 20°C/min, and a total reaction time of 80 minutes (annealed for 30 minutes) .....	58
Figure 53 SEM image 2 of graphene foam synthesized at 1000°C, ramping rate of 20°C/min, and a total reaction time of 80 minutes (annealed for 30 minutes) .....	59

Figure 54 SEM image 1 of graphene foam synthesized at 1000°C, ramping rate of 20°C/min, and a total reaction time of 95 minutes (annealed for 45 minutes) .....	59
Figure 55 Closeup image 1 of compressed graphene foam synthesized at 700°C, ramping rate of 10°C/min, and a total reaction time of 140 minutes (annealed for 70 minutes) .....	60
Figure 56 Closeup image 2 of compressed graphene foam synthesized at 700°C, ramping rate of 10°C/min, and a total reaction time of 140 minutes (annealed for 70 minutes) .....	61
Figure 57 Closeup image 1 of graphene foam synthesized at 800°C, ramping rate of 10°C/min, and a total reaction time of 140 minutes (annealed for 60 minutes).....	61
Figure 58 Closeup image 1 of graphene foam synthesized at 900°C, ramping rate of 10°C/min, and a total reaction time of 140 minutes (annealed for 50 minutes).....	62
Figure 59 Closeup image 2 of graphene foam synthesized at 900°C, ramping rate of 10°C/min, and a total reaction time of 140 minutes (annealed for 50 minutes).....	62
Figure 60 Closeup image 1 of graphene foam synthesized at 1000°C, ramping rate of 10°C/min, and a total reaction time of 140 minutes (annealed for 40 minutes).....	63
Figure 61 Closeup image 2 of graphene foam synthesized at 1000°C, ramping rate of 10°C/min, and a total reaction time of 140 minutes (annealed for 40 minutes).....	63
Figure 62 Closeup image 3 of graphene foam synthesized at 1000°C, ramping rate of 10°C/min, and a total reaction time of 140 minutes (annealed for 40 minutes).....	64
Figure 63 Closeup image 4 of graphene foam synthesized at 1000°C, ramping rate of 10°C/min, and a total reaction time of 140 minutes (annealed for 40 minutes).....	64
Figure 64 Closeup image 1 of graphene foam synthesized at 1000°C, ramping rate of 15°C/min, and a total reaction time of 140 minutes (annealed for 73 minutes).....	65
Figure 65 Closeup image 2 of graphene foam synthesized at 1000°C, ramping rate of 15°C/min, and a total reaction time of 140 minutes (annealed for 73 minutes).....	65
Figure 66 Closeup image 1 of graphene foam synthesized at 1000°C, ramping rate of 20°C/min, and a total reaction time of 140 minutes (annealed for 90 minutes).....	66
Figure 67 Closeup image 2 of graphene foam synthesized at 1000°C, ramping rate of 20°C/min, and a total reaction time of 140 minutes (annealed for 90 minutes).....	66
Figure 68 Closeup image 1 of graphene foam synthesized at 1000°C, ramping rate of 20°C/min, and a total reaction time of 65 minutes (annealed for 15 minutes).....	67

Figure 69 Closeup image 2 of graphene foam synthesized at 1000°C, ramping rate of 20°C/min, and a total reaction time of 65 minutes (annealed for 15 minutes)..... 67

Figure 70 Closeup image 1 of graphene foam synthesized at 1000°C, ramping rate of 20°C/min, and a total reaction time of 80 minutes (annealed for 30 minutes)..... 68

Figure 71 Closeup image 2 of graphene foam synthesized at 1000°C, ramping rate of 20°C/min, and a total reaction time of 80 minutes (annealed for 30 minutes)..... 68

Figure 72 Closeup image 1 of graphene foam synthesized at 1000°C, ramping rate of 20°C/min, and a total reaction time of 95 minutes (annealed for 45 minutes)..... 69

Figure 73 Closeup image 2 of graphene foam synthesized at 1000°C, ramping rate of 20°C/min, and a total reaction time of 95 minutes (annealed for 45 minutes)..... 69

## Table of Tables

Table 1 Breaks per 100 $\mu\text{m}^2$ in graphene foam synthesized at various annealing temperatures ..	22
Table 2 Ratio of breaks to intact strands per 100 $\mu\text{m}^2$ in graphene foam synthesized at various annealing temperatures .....	24
Table 3 Breaks per 100 $\mu\text{m}^2$ in graphene foam synthesized at various annealing times .....	28
Table 4 Ratio of breaks to intact strands per 100 $\mu\text{m}^2$ in graphene foam synthesized at various annealing times .....	29
Table 5 Breaks per 100 $\mu\text{m}^2$ in graphene foam synthesized at various ramping rates .....	33
Table 6 Ratio of breaks to intact strands per 100 $\mu\text{m}^2$ in graphene foam synthesized at various annealing times .....	34

# **Chapter 1: Scope of Work**

## **1.1 Initial Focus**

The initial focus of this project was to investigate the applicability of melamine-derived carbon foam as a thermal additive to absorbent crystals. Specifically, this material would be used in a water harvesting device. This material would be synthesized using pyrolysis. Its flexibility would be characterized using a scanning electron microscope (SEM), and its purity, which correlates to thermal conductivity, would be analyzed using Raman. The foam would be analyzed again using SEM after its saturation with absorbent crystals.

## **1.2 Shift in Focus**

Samples shipped off for Raman data yielded indiscernible data. Currently, we are in the process of purchasing our own Raman. However, purchasing delays prevented accurate data from being collected onsite. In addition, traveling followed by an upset in academic activities due to the COVID-19 disrupted data collection of SEM data. Alternative methods of data analysis were considered.

## **1.3 Final Focus**

The final focus of this project involves using literature review to assess the impact of different reaction conditions on the purity of the sample synthesized. In addition, a combination of qualitative and quantitative data was used to assess the flexibility of samples in order to compensate for a lack of quantitative data.

## **Chapter 2: Introduction**

### **2.1 Motivation**

Water scarcity affects over half of the world's population, and the population living in water scarcity is rapidly growing [1]. Current estimates state that roughly  $1.3 \times 10^{22}$  liters of water are stored in the Earth's atmosphere [2]. If this were accessible, it could serve to alleviate some of the population's water shortage. However, no practical methods of extracting water vapor from the atmosphere in arid climates, where water scarcity is particularly concerning, currently exist [3, 4]. Although attempts to construct a 'water harvester' to extract such water vapor have been made, the materials with which they are constructed limit their practicality [2-5]. Because of this, investigation into improved materials for use in such a device could yield positive progress in solving a global water crisis.

### **2.2 Background**

Many widely accepted processes are available for extraction of atmospheric water in high relative humidity climates [6-10]. However, practical solutions are needed for arid climates in which harvest of atmospheric water is difficult, as it must move up a concentration gradient for collection. This, therefore, requires an energy input [2].

A water harvester capable of operating at low relative humidity is composed of two major categories of materials: a thermally conductive material and an absorbent material [5]. The absorbent material is necessary to adsorb water vapor from the air, while the thermally conductive material encourages the desorption of the water in order for it to be collected for use [2]. Previous attempts to develop an effective device have used metal-organic frameworks (MOF) as absorbents and commercialized copper foam as a thermal additive to increase thermal conductivity. This has been effective in absorbing water from low relative humidity [2, 3, 5].

However, existing devices fail to meet necessary criteria for long term use, including low cost, scalability, and durability [4]. Therefore, the water harvester remains an impractical solution to the global water crisis until alternative materials are developed.

This project proposes the use of a novel melamine-derived graphene foam for use in a water harvester to create a cheap, lightweight, and durable alternative to current methods. Graphene has a documented ability to store thermal energy, and has flexible and lightweight properties which are necessary for the development of a water harvester, and graphene foams share these properties [11-13]. Graphene foam can be produced by pyrolysis of melamine foam, as shown in Chen et. al. [14]. In this reaction, nitrogen groups are released from melamine, and carbon-carbon double bonds form, leaving a web of interconnected phenol groups, or graphene [15, 16]. Carbon foam generated from this reaction has been shown to be lightweight, flexible, and highly thermally conductive [14, 17, 18]. Therefore, it has the potential to be an effective thermal conductor for use in water harvesting technology, while providing a solution to the problems associated with previous materials.

It should be noted that graphene foams, such as the one synthesized by Chen et al., are hydrophobic. In fact, they have proven to be effective in oil absorption [11, 14, 19-21]. Despite the potential advantages of using carbon foam, its lack of affinity for water creates a barrier in its use for water harvesting. Therefore, the use of graphene foam saturated with an absorbent has the great potential for use as an absorbent unit to enhance gravimetric and volumetric water harvesting efficiency. This project entails the synthesis and characterization of such a material.

Though this material has not previously been used for water harvesting purposes, the infiltration of hydrophobic carbon foam with absorbents has previously been performed by functionalizing the foam surface with strong acids and then saturated with a zeolite solution [22].

However, in order to develop a simpler and more scalable process, we have chosen to construct a zeolite-graphene foam composite without the use of functionalization. Instead, zeolites are dissolved in ethanol, and added to the foam. Ethanol was chosen as it is compatible with both polar and nonpolar substances, and therefore can both dissolve the hydrophilic zeolite particles, as well as infiltrate the hydrophobic graphene foam. Through trial and error, a zeolite which exhibits the closest packing within the pores of the graphene foam was selected. This was assessed qualitatively using Scanning Electron Microscope (SEM) imaging.

In addition to selection of a zeolite, the synthesis process of graphene foam was optimized in order to maximize its thermal conductivity and flexibility, which tend to be somewhat of a tradeoff in the synthesis process [14]. Thermal conductivity is believed to be correlated to graphene purity, which was assessed using Raman spectroscopy. Flexibility was assessed by analyzing SEM images before and after compressing the graphene foam.

## **Chapter 3: Methods and Materials**

### **3.1 Experimental Setup**

In order to develop an adequate environment in which to conduct the inert pyrolysis of melamine, a Lindberg/Blue Mini-Mite Tube Furnace Model TF55030A was chosen. Tube furnaces are able to rapidly heat a small area up to high temperatures. A quartz tube was specially cut to 30 cm for use inside the furnace. Quartz was chosen as it is stable at high temperatures. 1/8 inch copper piping was used to connect the exit valve of a tank containing Argon gas. A flow meter shown in Figure 1, which measured the precise volumetric flow rate of Argon gas entering the furnace.



**Figure 1** Flow meter

Argon gas then enters the quartz tubing inside of the tube furnace. Copper piping feeds the Argon gas exiting the quartz tubing into an appropriate waste stream. An image of this setup is shown in Figure 2.



**Figure 2** Lindberg/Blue Mini-Mite Tube Furnace and piping setup

Temperature inside of the furnace and the rate of heating or ramping rate were controlled using an Athena Series 16 Temperature/Process Controller shown in Figure 3.



**Figure 3** Athena XT16 Temperature/Process Controller

### 3.2 Pyrolysis Procedure

Graphene foam used in this process was produced by modifying a procedure from Chen et al [14]. Commercially available melamine foam was heated under an argon atmosphere for a period of time. An inert atmosphere is necessary for this reaction, as melamine will burn under standard atmosphere.

Each sample was prepared by inserting a 1 cm X 1 cm X 0.5 cm piece of melamine foam into the center of the Lindberg/Blue Mini-Mite Tube Furnace Model TF55030A. Before turning the furnace on, argon gas was allowed to flow through the furnace for 30 minutes to flush out any air within the furnace or within the pores of the samples. Using the Athena XT16 Temperature/Process Controller to regulate the rate of heating and overall temperature of the reaction, an annealing temperature and rate of heating (ramping rate) was set and the furnace was turned on. The sample was the allowed to rest at the annealing temperature for a certain amount of time before the furnace was shut off and allowed to cool on its own. At the time that the furnace was turned off, argon gas flow was shut off and the furnace was sealed, allowing no air in. Once cooled, the sample was removed from the furnace and prepared for analysis.

Previous research has investigated the effect of temperature on product purity. However, few studies provide quantitative data connecting the annealing temperature of the pyrolysis reaction to the flexibility of the final sample. In addition, no studies analyze the effects of other reaction conditions, including the ramping rate or annealing time on the overall purity of the product and its mechanical properties. Therefore, in this study, we chose to modify the reaction conditions in order to test each of these parameters.

Annealing temperatures between 700, 800, 900, and 1000°C were synthesized at a constant reaction time of 140 minutes and a ramping rate of 10°C/min. Results from these were compared in order to analyze the effect of annealing temperature on sample flexibility and purity. Similarly, annealing times of 15, 30, 40, and 45 minutes were compared. Each of these samples was synthesized at 1000°C with a ramping rate of 20°C/min. Ramping rates of 10, 15, and 20°C/min were compared using samples synthesized at 1000°C with a total reaction time of 140 minutes.

### 3.3 Mechanical Strength Characterization

In order to compare mechanical strength of samples, a Hitachi S3400 scanning electron microscope (SEM) was used. Graphene foam cross-sections were loaded onto the SEM stubs using double-sided carbon tape. This allowed us to see the surface of samples. Images were taken of each sample before and after compressing the sample. In doing so, we were able to gain a qualitative comparison of the mechanical properties of each sample. Each sample of graphene foam consists of an interlocking web of strands roughly 1  $\mu\text{m}$  thick as shown in Figure 4.

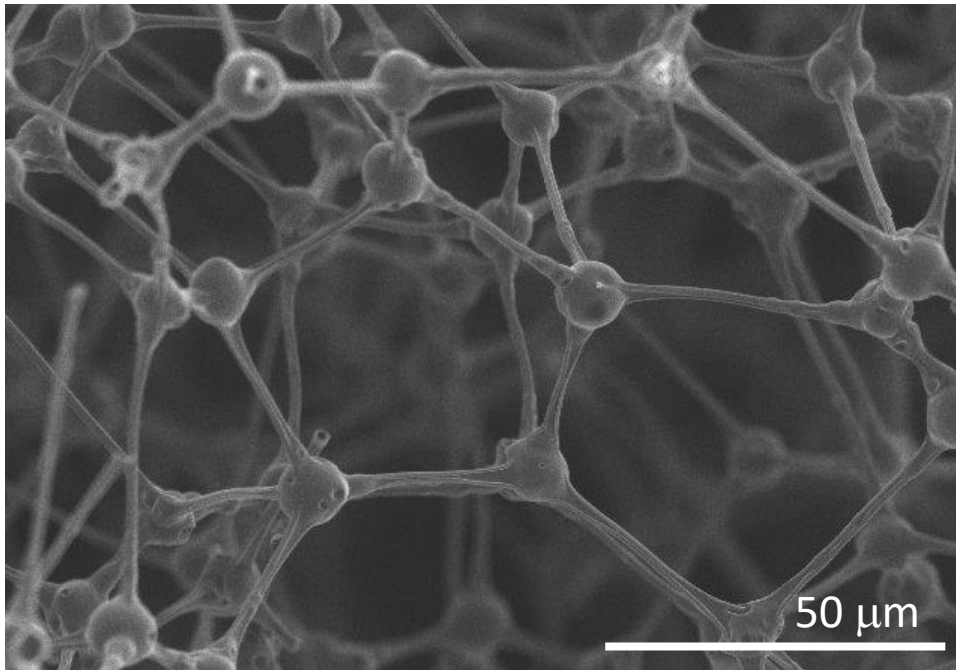


**Figure 4** Graphene foam structure

When the foam is compressed, it is damaged. Individual strands will break or become otherwise deformed. The sample shown in Figure 4 can be seen after compression in Figure 5.

Observing differences in structure following compression in different samples can provide insight into the mechanical strength of the samples.

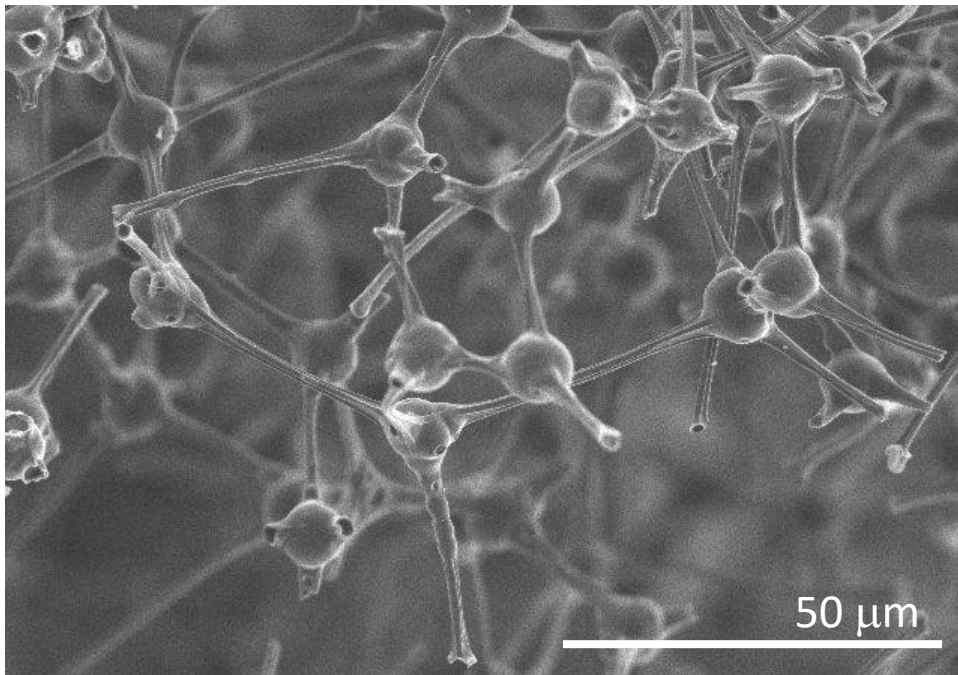


**Figure 5** Graphene foam structure after compression

In order to perform a qualitative analysis of the mechanical strength of each sample, ImageJ software was used. ImageJ is a software that allows you to perform detailed analysis of images taken using a microscope. In this case, ImageJ software was used to create a 100 μm square on each image analyzed. This can be seen in Figure 6.

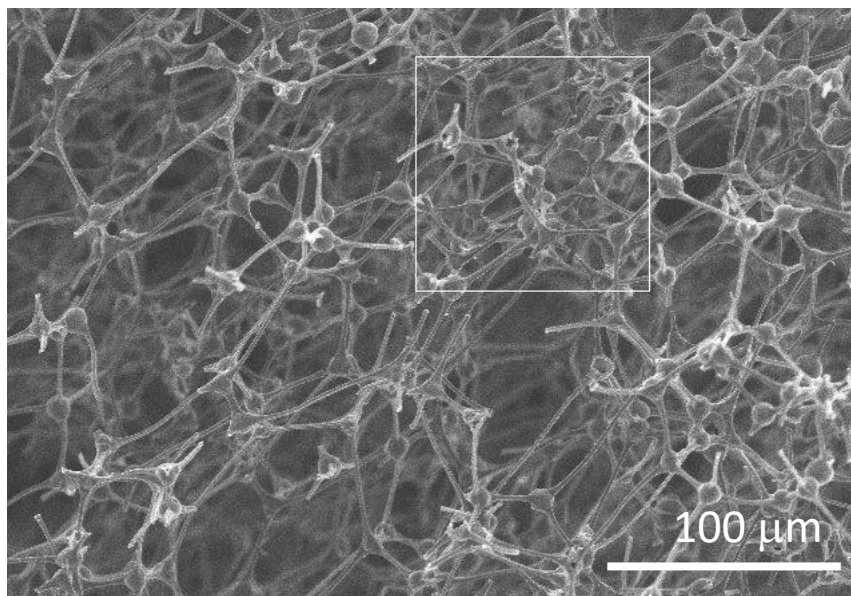


**Figure 6** Area selected for analysis

The number of breaks per  $100 \mu\text{m}^2$  in each compressed sample was counted for all valid images. These results were averaged over multiple images, and a 95% confidence interval for the number of breaks per  $100 \mu\text{m}^2$  calculated using a student's t-test. From this, results were plotted and conclusions about the mechanical strength and flexibility of each sample were drawn. It was assumed that samples with fewer breaks after compression were more flexible than those with more breaks. In addition, to account for variations in images, the ratio of broken strands to intact strands was also compared.

### **3.4 Raman Spectroscopy**

Raman spectroscopy can be used to assess the composition of materials. Therefore, it can be used to determine the purity of a material. This can be done by considering the different absorption bands. Critical bands for consideration in graphene are the D band at roughly 1300

cm<sup>-1</sup> and the G band at roughly 1600 cm<sup>-1</sup> [23, 24]. A decrease in width of these two bands, yielding sharper peaks, is considered to be evidence of a more fully carbonized foam [14, 19].

In order to study the effects of the chosen variables on the final composition, samples were shipped to a facility for Raman spectroscopy data to be obtained. In addition, literature review was used to supplement acquired data.

### **3.5 Addition of Zeolites**

Graphene foam in this project is set to act as a thermal additive to zeolites in order to increase their thermal conductivity. Zeolites used in this project include 13X, produced by Sigma-Aldrich and Z-02, produced by AQSOA, Mitsubishi. In order for them to be used in this manner, it is necessary to develop a procedure for the saturation of the pores of graphene foam with zeolites. Closest packing possible of the zeolite material is important as the more zeolite, the more water that the material is able to absorb.

Rather than functionalizing the surface of graphene foam to make it more hydrophilic, organic solvents were used to dissolve the zeolites. A 60% solution of zeolite powder in ethanol was made. The graphene foam sample was added to this solution and compressed, forcing it to take up the solution in its pores. The samples were then dried in an oven at 60°C for several hours. The samples were then removed from the oven and prepared for testing.

A number of different zeolites were used for testing in this process. The two that displayed the best packing when left to settle in water were compared. SEM was used to examine how well the zeolites packed the pores of the graphene foam following their addition.

## Chapter 4: Results and Discussion

### 4.1 Mechanical Strength and Flexibility

The flexibility of each sample was analyzed using the procedure described in section 3.3. Results are presented in tabular and graphical format for each set of trials (varying annealing temperature, annealing time, and ramping rate) for both the overall number of broken strands found as well as the ratio of broken strands to intact strands. Error bars on graphs display a 95% confidence interval. Data points without error bars shown only had one piece of data, so a confidence interval could not be calculated.

#### 4.1.1 Effect of Annealing Temperature

Shown in Table 1 and Figure 7 are the results from counting the number of breaking points per  $100 \mu\text{m}^2$  when varying the annealing temperature.

**Table 1** Breaks per  $100 \mu\text{m}^2$  in graphene foam synthesized at various annealing temperatures

Annealing Temperature (°C)	Breaks per $100 \mu\text{m}^2$						Percentage Error
	Trial 1	Trial 2	Trial 3	Trial 4	Mean	95% Confidence Interval	
700	15	20	22	18	18.75	6.4	34.3
800	12	14	-	-	13	4.3	33.1
900	25	-	-	-	25	n/a	n/a
1000	24	-	-	-	24	n/a	n/a

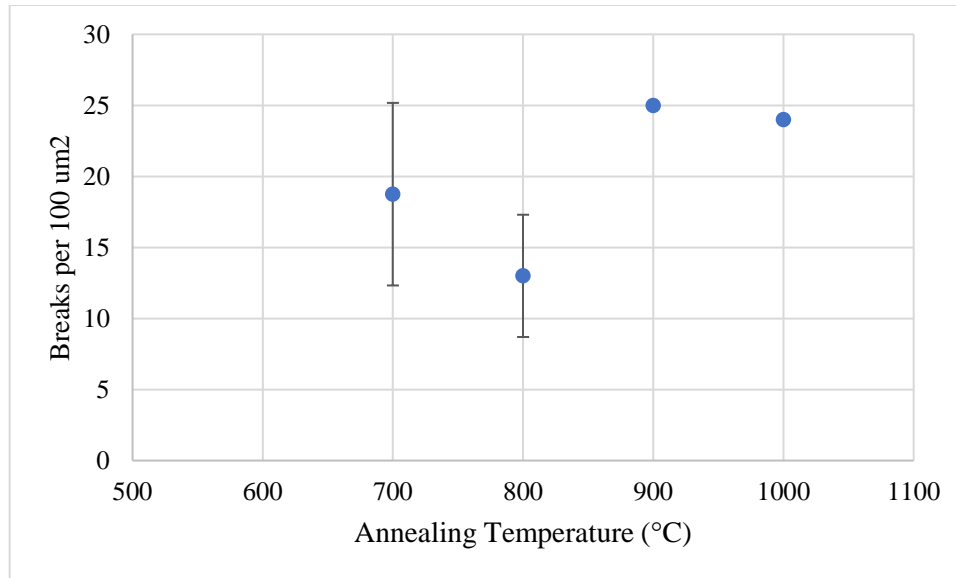


**Figure 7** Breaks per 100  $\mu\text{m}^2$  in graphene foam synthesized at various annealing temperatures

From Table 1 and Figure 7, it appears that an annealing temperature of 800 °C tends to be the most flexible out of all annealing temperatures tested. The samples synthesized at higher annealing temperature (900 and 1000°C) are the least flexible, taking the most damage following compression. It should be noted that the margin of error for this data is relatively large. This is likely due to the limited number of trials conducted. If a larger number of samples were to be analyzed, the confidence interval would shrink considerably. However, due to issues accessing lab equipment due to the campus shutdown caused by COVID-19, additional data could not be obtained in the timeframe necessary to complete this project.

Another potential reason for the large margin of error was thought to be density of strands in focus. If an area in focus of the SEM were to contain fewer strands in general, the number of broken strands would be much smaller in comparison to other in other images. In order to combat this bias, the ratio of breaks in strands to the overall number of intact strands within the region analyzed was calculated. Results from this are shown in Table 2 and Figure 8.

**Table 2** Ratio of breaks to intact strands per 100  $\mu\text{m}^2$  in graphene foam synthesized at various annealing temperatures

Annealing Temperature (°C)	Breaks: Intact Strands					95% Confidence Interval	Percentage Error
	Trial 1	Trial 2	Trial 3	Trial 4	Mean		
700	1.0	1.4	1.2	0.6	1.1	0.7	69.0
800	0.6	1.1	-	-	0.8	1.0	122.4
900	1.0	-	-	-	1.04166667	n/a	n/a
1000	1.3	-	-	-	1.26315789	n/a	n/a

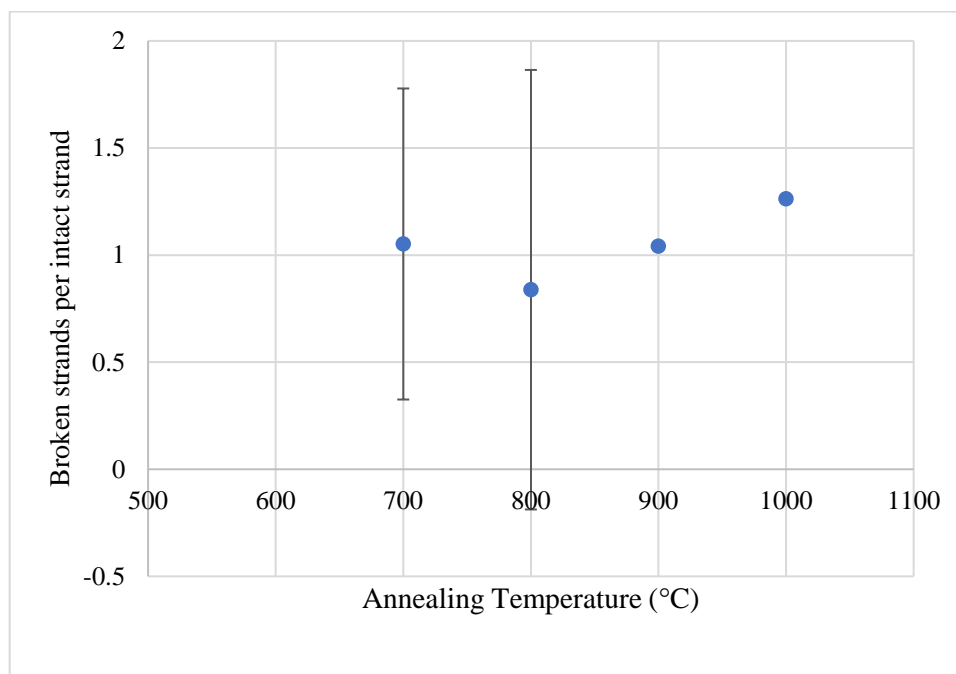


**Figure 8** Ratio of breaks to intact strands per 100  $\mu\text{m}^2$  in graphene foam synthesized at various annealing temperatures

From Table 2 and Figure 8, the results appear to correlate to what was found in Table 1 and Figure 7. However, the margin of much error is even higher. The high margin of error is, once again, likely due to the small range of data collected.

Therefore, from the data collected, we can assume with caution that an ideal annealing temperature for this process in order to maximize flexibility is roughly 800°C, with higher temperatures exhibiting particularly low flexibility. Further data collection should be done in order to reduce the error associated with these results. However, it seems reasonable to accept these results as qualitative data appears to support these findings. Shown in Figure 9-Figure 12 are images of individual strands of each sample following compression. Images were chosen which were considered for display in this section which were considered to be characteristic of the entire sample. Additional images can be found in Appendix 3.

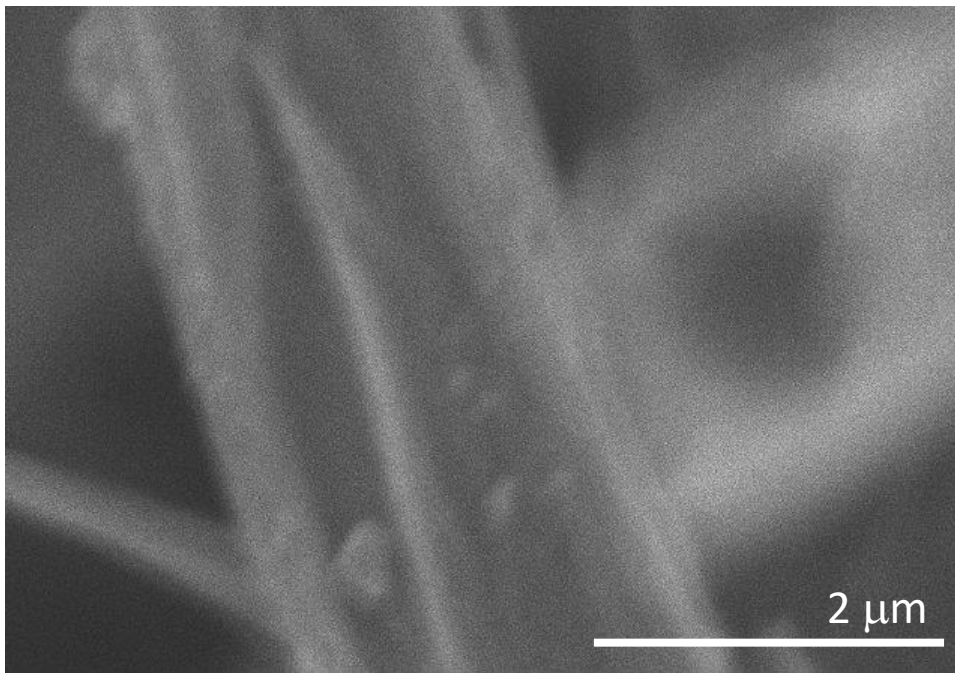


**Figure 9** Graphene foam synthesized at 700°C following compression

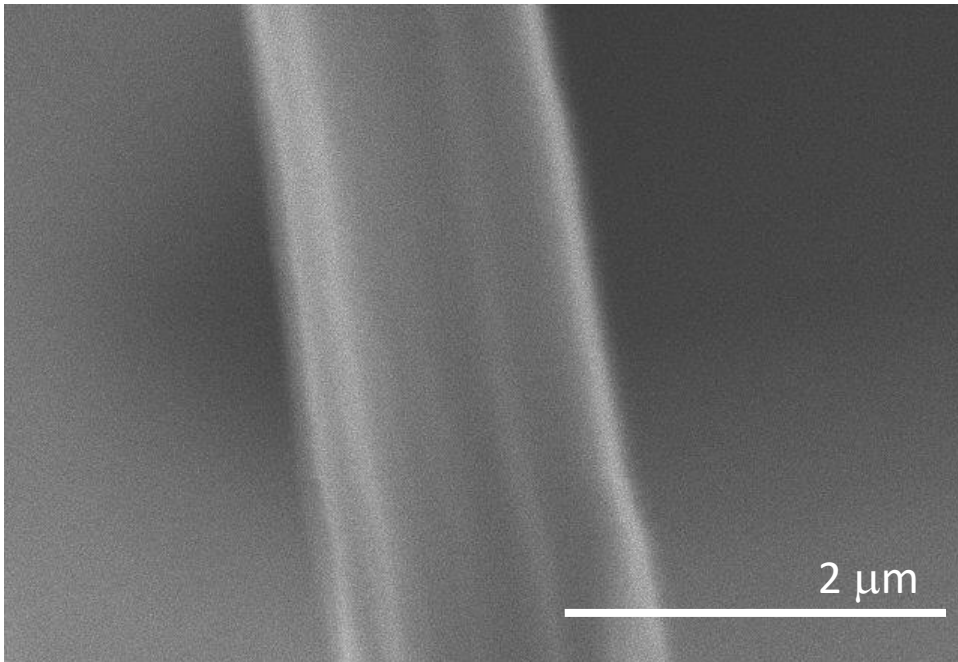


**Figure 10** Graphene foam synthesized at 800°C following compression

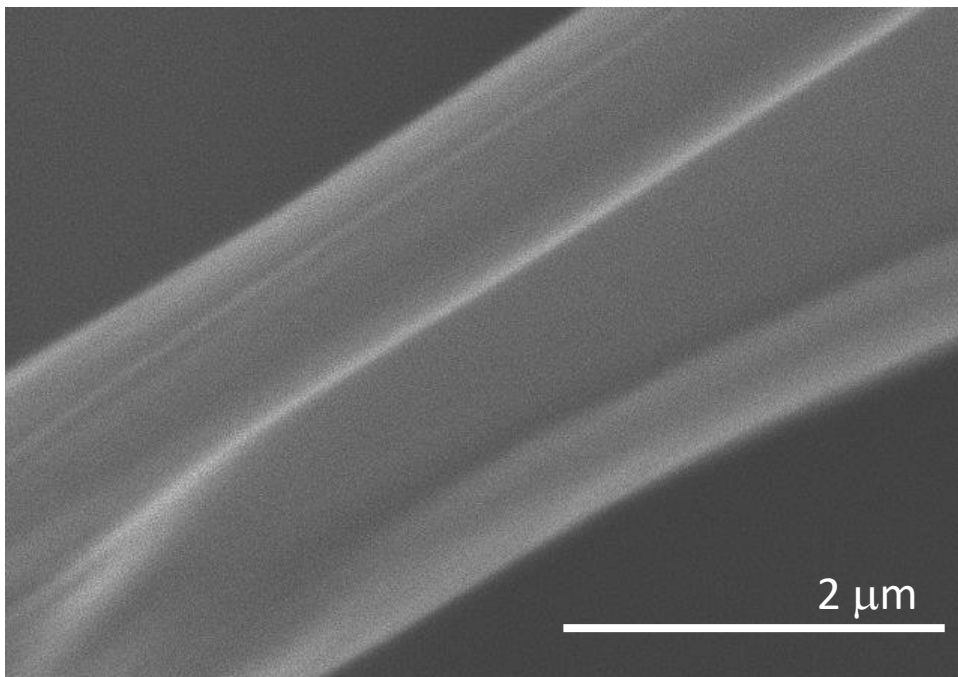


**Figure 11** Graphene foam synthesized at 900°C following compression

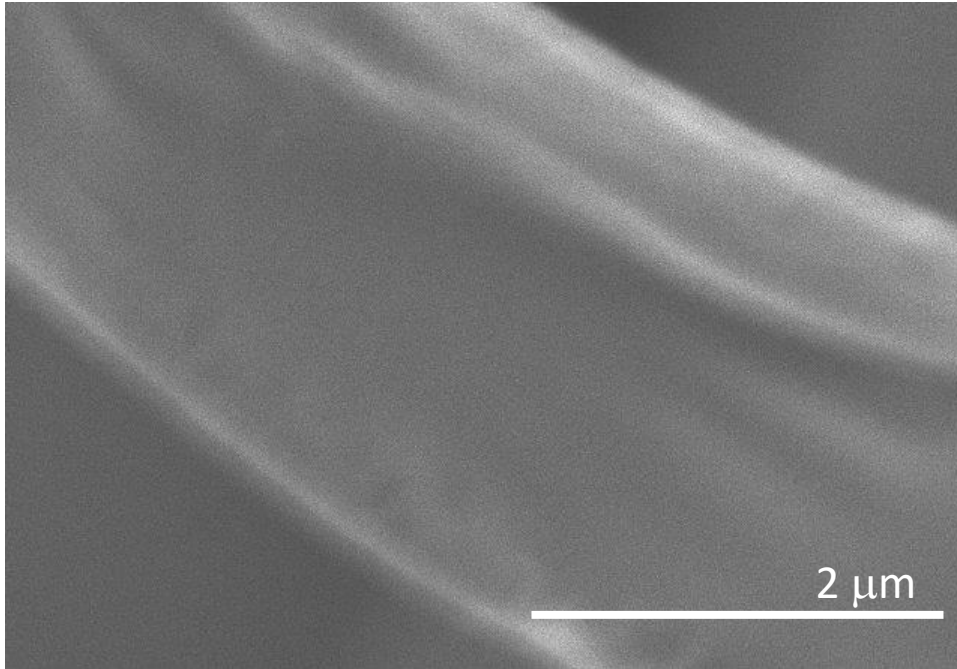


**Figure 12** Graphene foam synthesized at 1000°C and ramping rate of 10°C/min following compression

From Figure 9, the physical deformities in this strand of graphene synthesized at 700°C are evident. The surface appears to be jagged and sharp, rather than smooth. This could indicate that damage has been taken by this sample following compression. From Figure 10 and Figure 11, samples synthesized at 800 and 900°C are much smoother and uniform, with few visible physical deformities, indicating that they have taken less damage from being compressed than the other samples. From Figure 12, the sample synthesized at 1000°C has a small amount of cracking on its surface and its strand appears to be curved. This indicates that it has been damaged in some way. Therefore, qualitative analysis of Figure 9-Figure 12 support the conclusion drawn from Figure 7-Figure 8 and Table 1-Table 2 that graphene foam synthesized at 800°C is stronger than graphene foam synthesized at other annealing temperatures.

#### 4.1.2 Effect of Annealing Time

A similar analysis was performed for samples of varying annealing times. Shown in Table 3 and Figure 13 are the results from counting the number of breaking points per  $100 \mu\text{m}^2$  when varying the annealing temperature.

**Table 3** Breaks per  $100 \mu\text{m}^2$  in graphene foam synthesized at various annealing times

Annealing Time (min)	Breaks per $100 \mu\text{m}^2$						Mean	95% Confidence Interval	Percentage Error
	Trial 1	Trial 2	Trial 3	Trial 4	Trial 5	Trial 6			
90	38	8	10	21	11	15	17.2	19.7	114.6
15	15	6	12	17	20	29	16.5	13.6	82.7
30	30	23	-	-	-	-	26.5	15.1	56.8
45	25	-	-	-	-	-	25.0	n/a	n/a

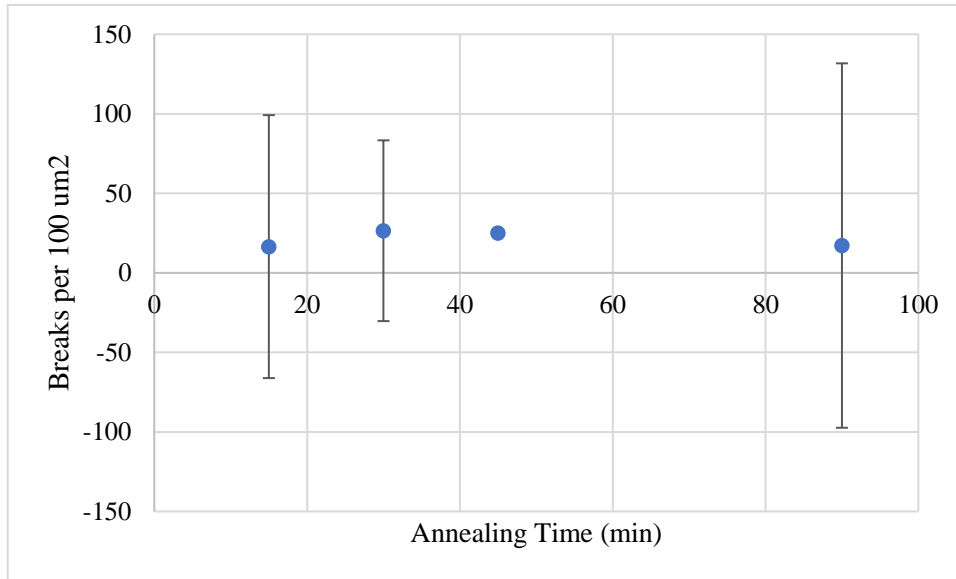


**Figure 13** Breaks per  $100 \mu\text{m}^2$  in graphene foam synthesized at various annealing times

From Table 3 and Figure 13, annealing time does not appear to have a significant effect on the overall flexibility of the graphene foam, as the number of breaks per 100  $\mu\text{m}^2$  is similar despite variation in annealing time. A slight peak at 45 minutes of annealing occurs. Results from calculating the ratio of broken strands to intact strands are shown in Table 4 and Figure 14.

**Table 4** Ratio of breaks to intact strands per 100  $\mu\text{m}^2$  in graphene foam synthesized at various annealing times

Annealing Time (min)	Breaks: Intact Strands						Mean	95% Confidence Interval	Percentage Error
	Trial 1	Trial 2	Trial 3	Trial 4	Trial 5	Trial 6			
90	2.4	0.7	1.0	1.0	0.48	0.79	1.04	1.19	114.33
15	2.2	1.9	0.6	0.5	0.55	0.94	1.12	1.34	119.56
30	1.7	1.0	-	-	-	-	1.36	1.34	98.55
45	1.9	-	-	-	-	-	1.92	n/a	n/a

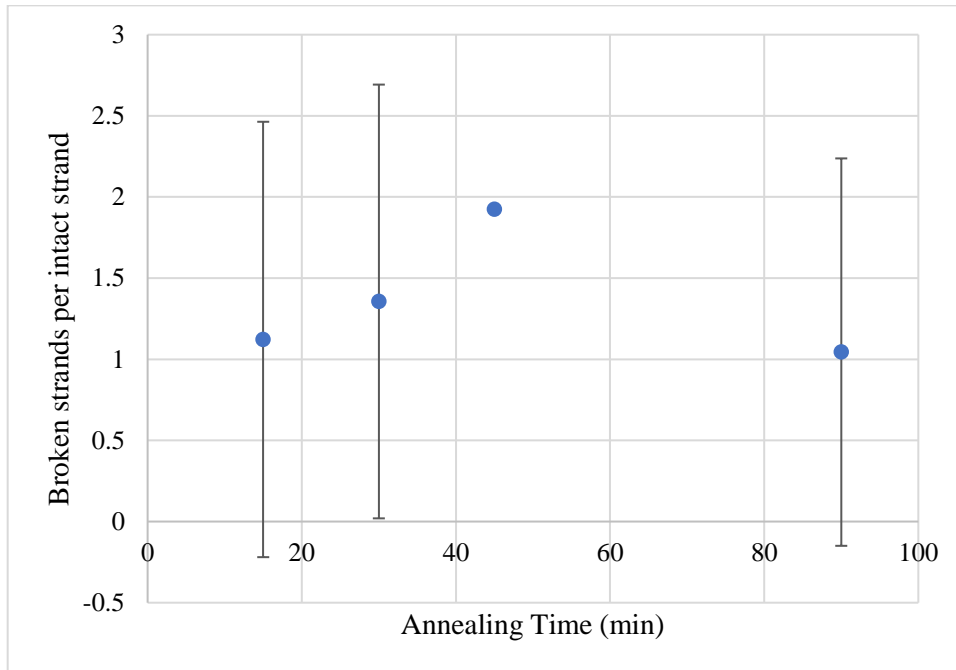


**Figure 14** Ratio of breaks to intact strands per 100  $\mu\text{m}^2$  in graphene foam synthesized at various annealing times

From Table 4 and Figure 14, the peak at 45°C is slightly higher than that in Table 3 and Figure 13. Therefore, from analyzing the number of breaks per 100  $\mu\text{m}^2$  and the ratio of breaks to intact strands, it can be assumed that annealing time has a slight effect on flexibility, but it may be somewhat insignificant. It should be noted that only one data point was collected for an annealing time of 45°C. Therefore, the confidence interval could not be calculated. If more data were to be collected, it is likely that we would see the peak that occurs at 45°C flatten out.

The effect of annealing time was assessed qualitatively as well. Shown in Figure 15- Figure 18 are images of individual strands of each sample following compression.

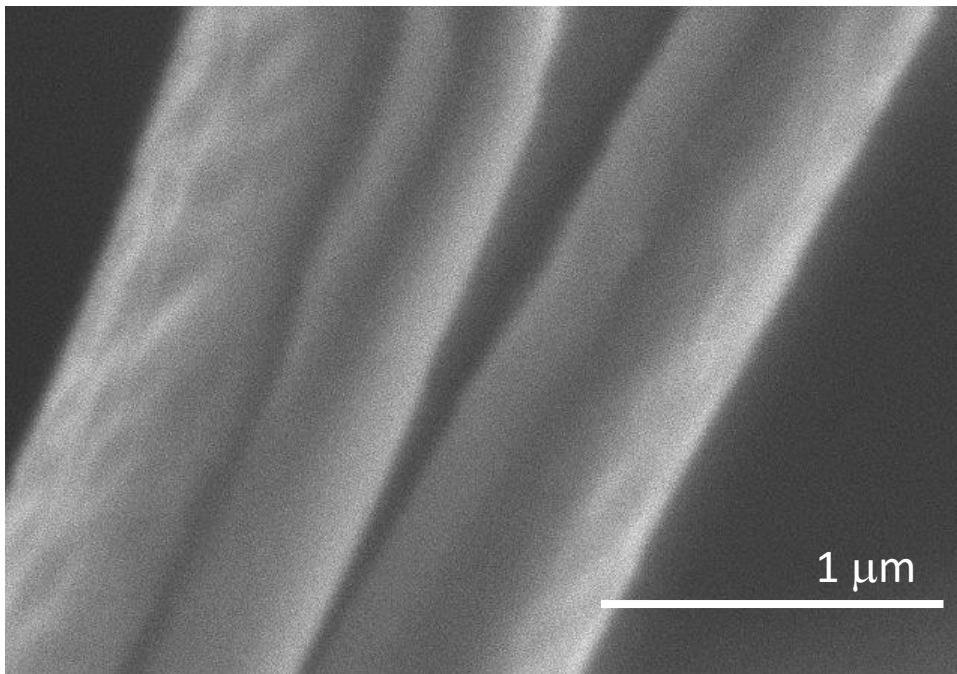


**Figure 15** Graphene foam annealed for 90 minutes with ramping rate of 20°C/min then compressed

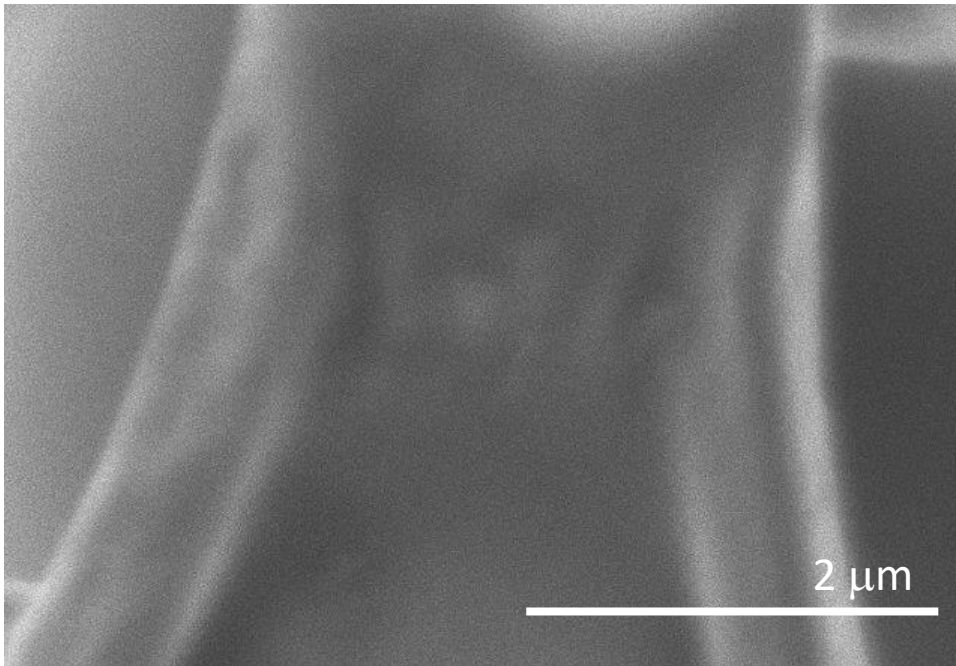


**Figure 16** Graphene foam annealed for 15 minutes then compressed

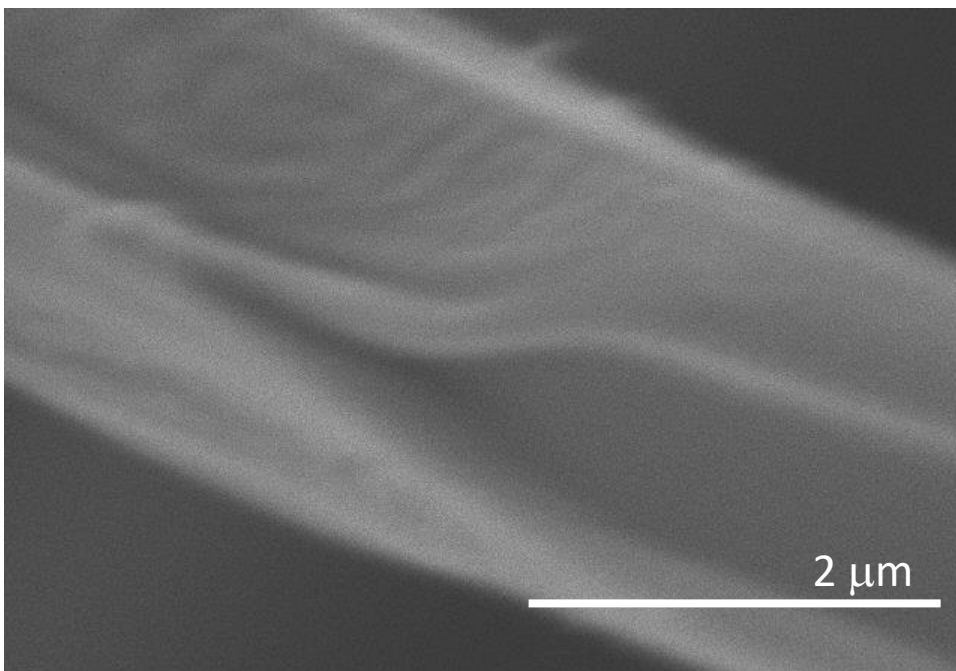


**Figure 17** Graphene foam annealed for 30 minutes then compressed

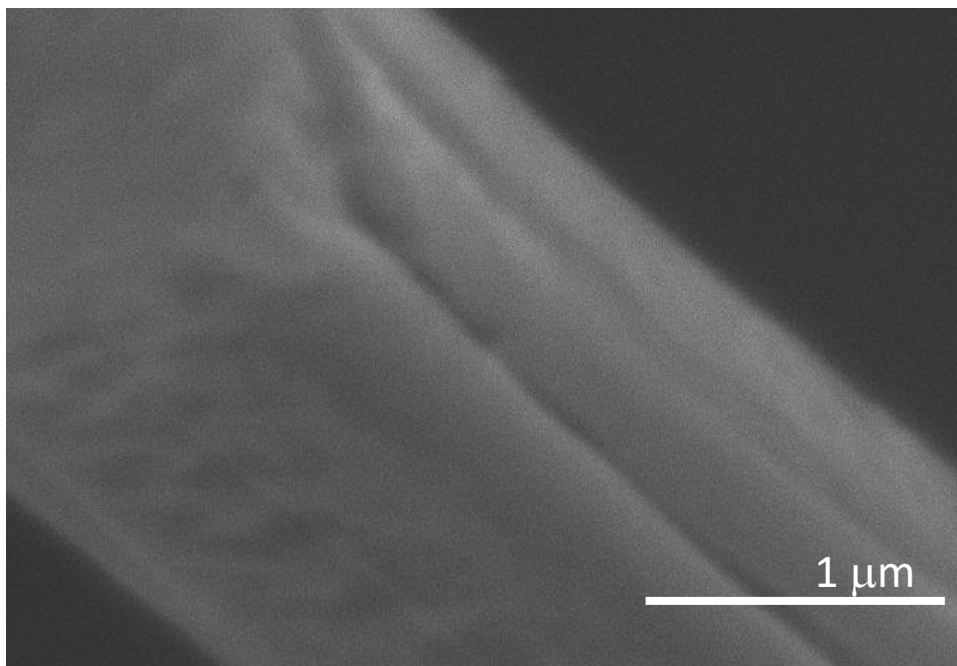


**Figure 18** Graphene foam annealed for 45 minutes then compressed

From Figure 15-Figure 18, all samples appear to exhibit similar damage. Each sample has moderate cracking and deformation on its surface. This supports the findings in Table 3 and Figure 13 as there appears to be no significant difference in flexibility of the samples annealed for different lengths of time. Therefore, it is reasonable to consider the peak at 45 minutes annealing time in Table 4 and Figure 14 to be the result of a lack of additional trials.

Given that the annealing time has little effect on the flexibility of the sample, it may be reasonable to shorten the annealing time for the sake of accelerating the speed of lab work. Alternately, if the annealing time has a positive correlation to product purity, a longer annealing time could be used increase purity while maintaining flexibility.

### 4.1.3 Effect of Ramping Rate

Again, a similar analysis was performed to determine the effect of ramping rate on sample flexibility. Shown in Table 5 and Figure 19 are the results from counting the number of breaking points per 100  $\mu\text{m}^2$  when varying the ramping rate.

**Table 5** Breaks per 100  $\mu\text{m}^2$  in graphene foam synthesized at various ramping rates

Ramping Rate ( $^{\circ}\text{C}/\text{min}$ )	Breaks per 100 $\mu\text{m}^2$						Mean	95% Confidence Interval	Percentage Error
	Trial 1	Trial 2	Trial 3	Trial 4	Trial 5	Trial 6			
10	24	-	-	-	-	-	24.0	n/a	n/a
15	25	27	15	16	18	-	20.2	10.5	51.9
20	38	8	10	21	11	15	17.2	19.7	114.6

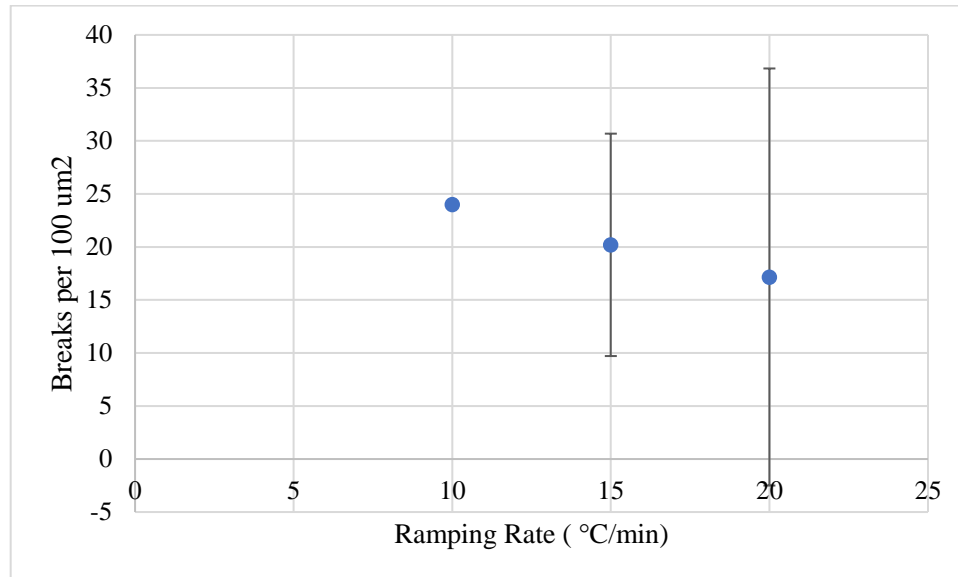


**Figure 19** Breaks per 100  $\mu\text{m}^2$  in graphene foam synthesized at various ramping rates

From Table 5 and Figure 19, there appears to be an inverse relationship between ramping rate and sample flexibility. The ratio of broken strands to intact strands was assessed in Table 6 and Figure 20.

**Table 6** Ratio of breaks to intact strands per 100  $\mu\text{m}^2$  in graphene foam synthesized at various annealing times

Ramping Rate ( $^{\circ}\text{C}/\text{min}$ )	Breaks: Intact Strands						Mean	95% Confidence Interval	Percentage Error
	Trial 1	Trial 2	Trial 3	Trial 4	Trial 5	Trial 6			
10	1.3	-	-	-	-	-	1.26	0.00	0.00
15	1.5	1.5	1.4	1.1	1.29	-	1.35	0.28	20.64
20	2.4	0.7	1.0	1.0	0.48	0.79	1.04	1.19	114.33

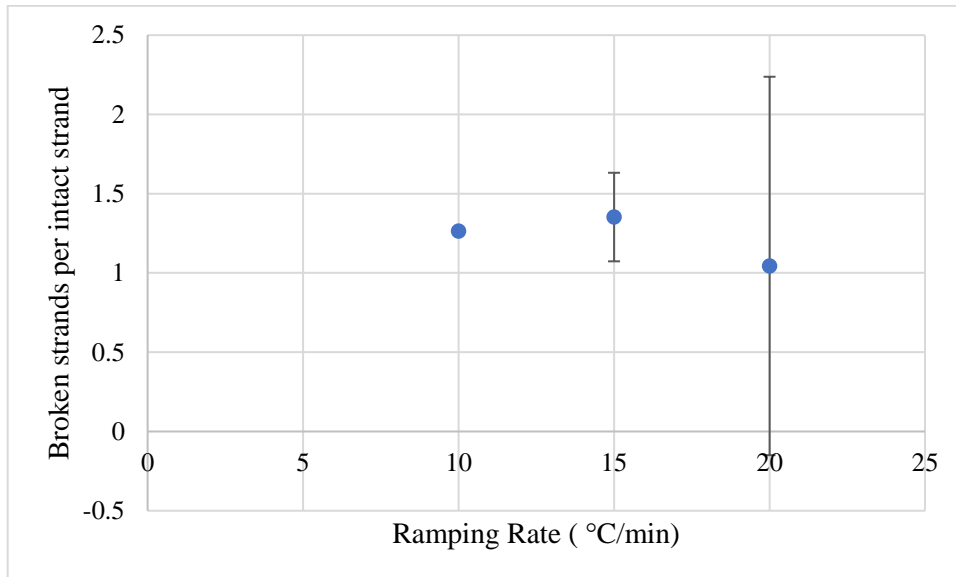


**Figure 20** Ratio of breaks to intact strands per 100  $\mu\text{m}^2$  in graphene foam synthesized at various annealing times

Unlike in Table 5 and Figure 19, Table 6 and Figure 20 do not indicate a distinct downward trend. However, given the size of the error bars and the fact that the mean value for

the highest ramping rate (20°C/min) was significantly lower than the other two values, it is likely that such a downward trend may exist. Images of samples synthesized at ramping rates of 10 and 20°C/min have been shown in previous sections of this report. They can be found in Figure 12 and Figure 15 respectively. An image of a sample synthesized at a ramping rate of 15°C/min can be seen in Figure 21.

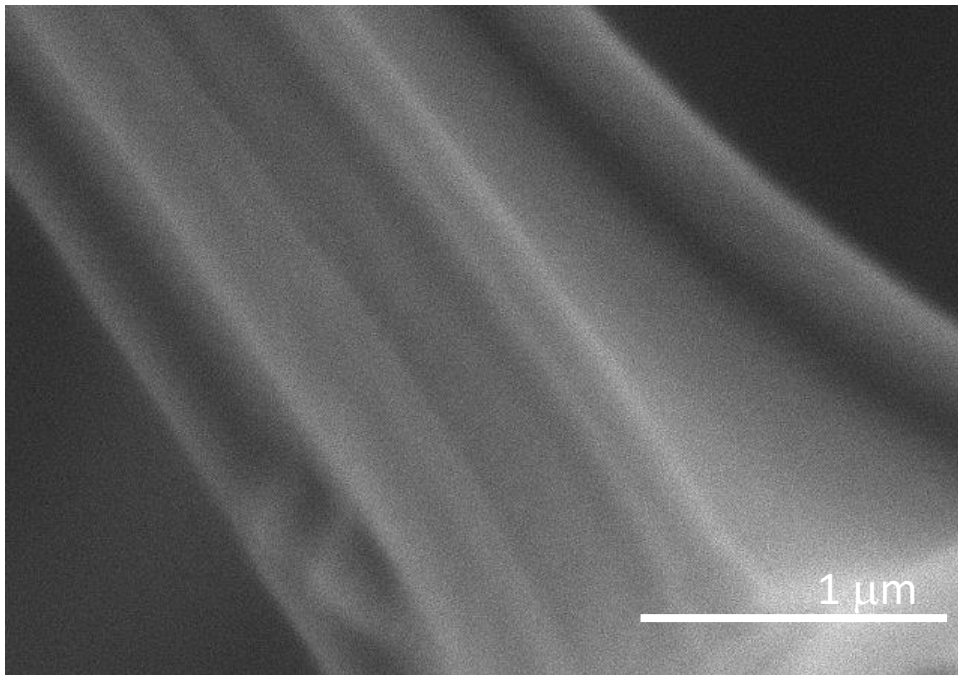


**Figure 21** Graphene foam synthesized at a ramping rate of 15°C/min after compression

From Figure 12, Figure 15, and Figure 21, the sample appears the most damaged at a ramping rate of 20°C/min and the least damaged at a ramping rate of 10°C/min. This contradicts the trend in Table 5 and Figure 19, as well as the lack of a trend in Table 6 and Figure 20. Because of the wide range of trends seen in the data surrounding ramping rate, the study of the effect of ramping rate on product flexibility can be considered to be inconclusive.

## 4.2 Raman Spectroscopy and Literature Review

Raman spectroscopy data for samples synthesized at various annealing temperatures, annealing times, and ramping rate is shown in Figure 22-Figure 24.

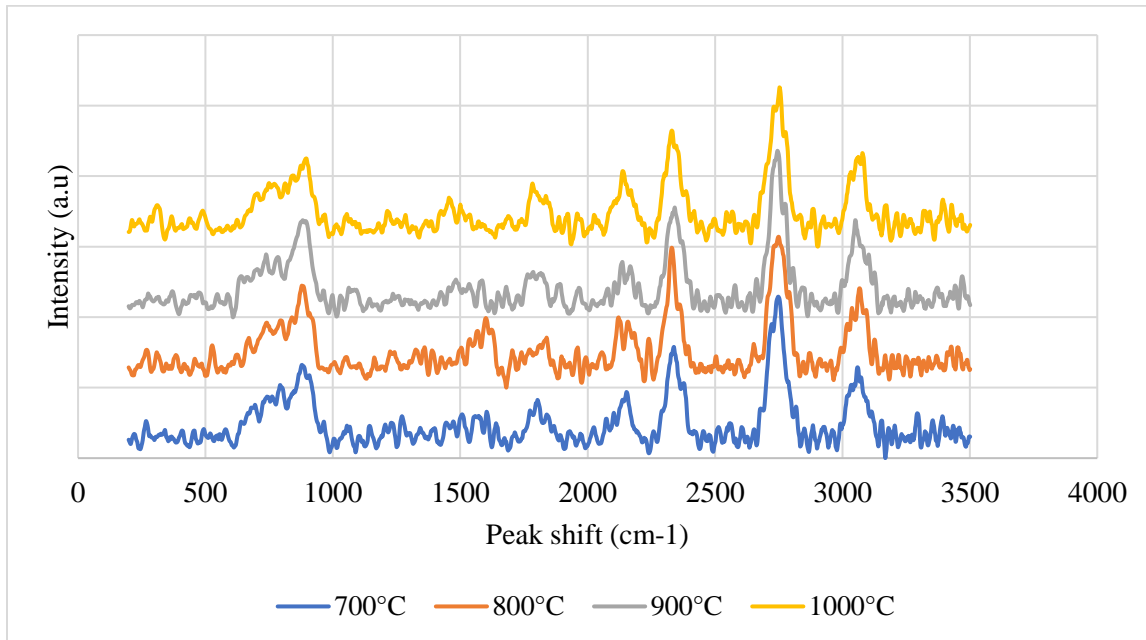


**Figure 22** Raman spectroscopy of graphene foam synthesized at various annealing temperatures

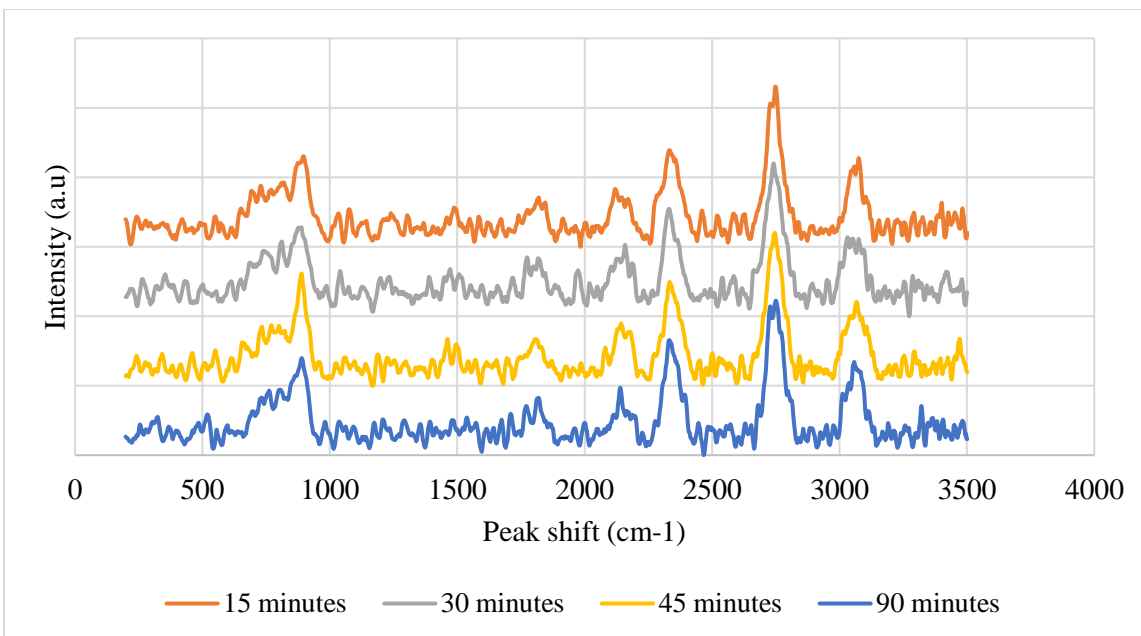


**Figure 23** Raman spectroscopy of graphene foam synthesized at various annealing times

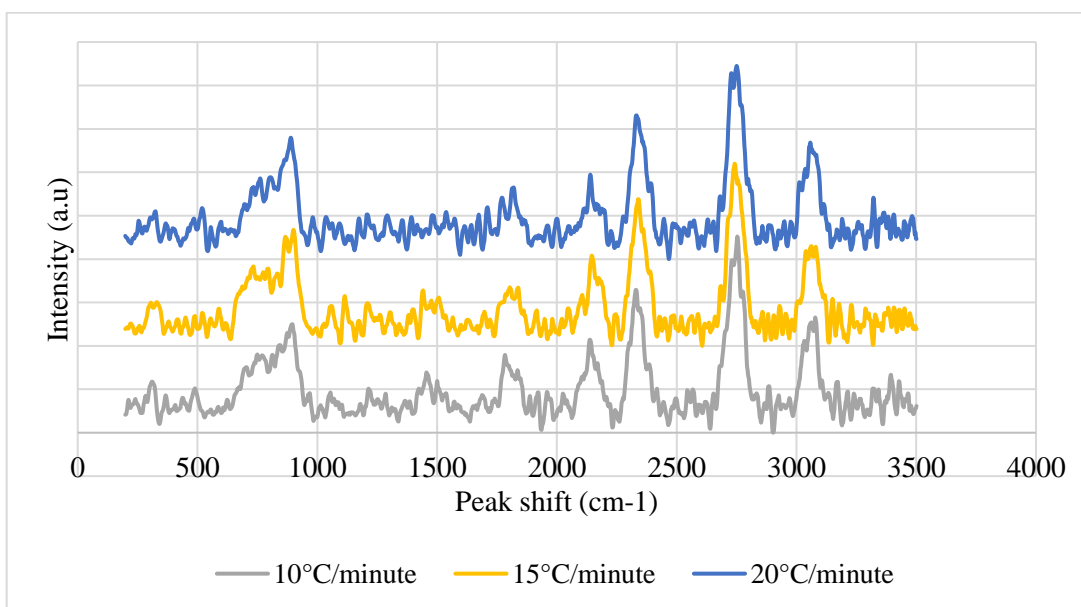


**Figure 24** Raman spectroscopy of graphene foam synthesized at various ramping rates

From Figure 22-Figure 24, no discernable bands appear for any sample analyzed. This is likely due to experimental error. Considering the lack of insight that this data brings, it is best to resort to literature review until further accommodations can be made.

Current research suggests that sharper peaks at the D-band and G-band occur when graphene foam is annealed at higher temperatures [14, 19]. Chen et. al. suggests that the purity of samples synthesized at temperatures between 700°C and 1000°C does not vary significantly. At much higher temperatures, such as 1800°C a notable difference in product composition can be seen [14]. However, synthesis at such high temperatures is impractical for the purposes of this project, as the flexibility of the graphene foam is significantly reduced.

Therefore, it can be reasonably assumed based on literature values that graphene foam samples have a higher purity when synthesized at higher temperatures. The effect of other parameters tested could not be found in literature. However, as they seemed to have a negligible effect on the flexibility of the samples, it may seem reasonable to consider them negligible to the overall product composition as well, until further data can be collected. From the data generated in section 4.1 and 4.2, it appears that flexibility and foam purity are inversely related. Therefore, a compromise must be reached between the two parameters. In general, it appears that an annealing temperature of 800°C produces a highly flexible foam, with an adequate purity. Therefore, it is reasonable that we use this annealing temperature moving forward.

### **4.3 Addition of Zeolite**

Graphene foam-zeolite composites were synthesized according to the procedure in section 3.5. This procedure was tested using two different varieties of zeolites, known

commercially as Z-02 and 13X. SEM images taken of the two composites can be seen in Figure 25 and Figure 26.

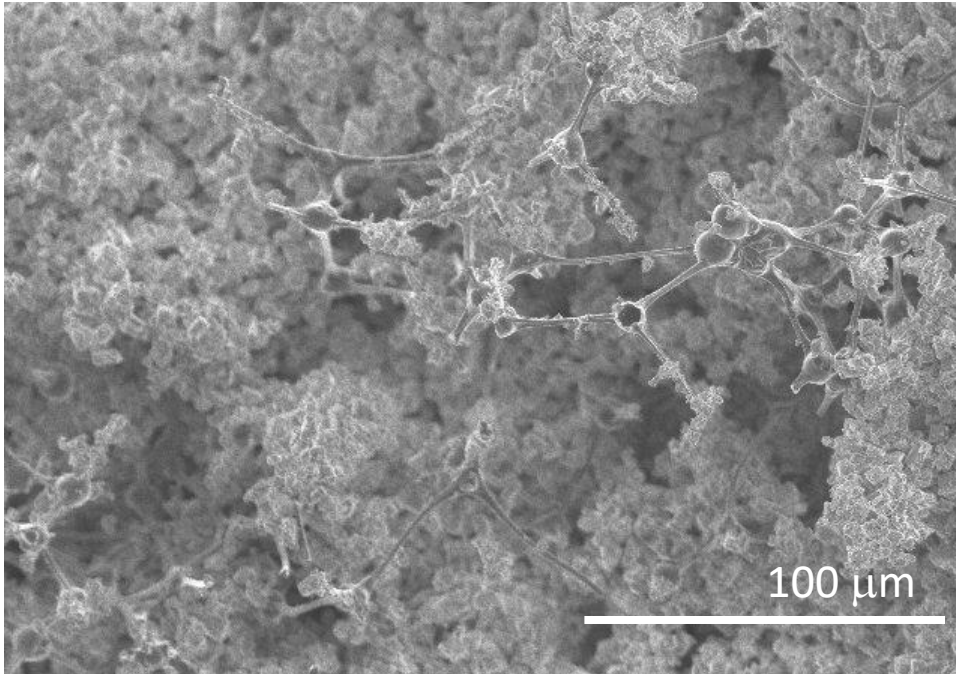


**Figure 25** Graphene foam saturated with Z-02

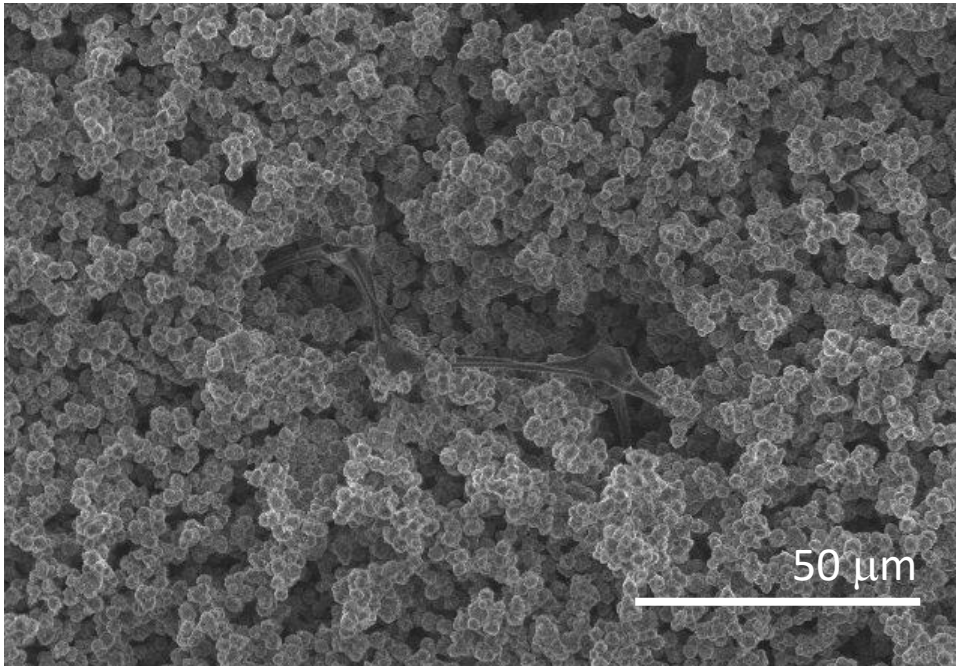


## **Figure 26** Graphene foam saturated with 13X

From Figure 25, Z-02 forms a relatively loose packed. Empty pores of graphene can be seen. However, in Figure 26, 13X forms a much tighter packing. Strands of graphene foam can be seen attached to zeolite particles. Therefore, 13X is much better for use in this material than Z-02 as it forms a tighter packing when added to graphene foam.

### **4.4 Potential Sources of Error**

As previously stated, the small number of trials utilized during flexibility testing may be led to larger errors than are ideal. Increasing the number of trials performed may have corrected this issue. Selection of a region to analyze on SEM images could have been somewhat biased due to human error. A larger sample size would lessen the effects of this as well.

In addition, samples were compressed manually with a chemical spatula, rather than with a machine that could have regulated pressure more accurately. Had a device which could regulate the pressure applied been used, this test could have been more accurate as well. In this future, this experiment may be repeated using a device rather than doing this by hand. In addition, a device which will allow for the compression of each sample by machine has been 3D printed. Graphene can be inserted into a pocket within the device and a piston can be inserted, compressing the sample vertically.

Qualitative assessment of zeolite packing is not as accurate as quantitative data. There may be bias in image selection or of region analyzed. This could lead to inaccurate results.

Using Raman data not specific to our samples may not be accurate as well, due to variations in experimental techniques. This concern will be alleviated in the future when our lab group obtains the proper equipment in order to evaluate our own samples.

## **Chapter 5: Conclusions**

### **5.1 Conclusion and Recommendations**

Graphene foam was found to be the most flexible when annealed at 800°C. Annealing time had no effect on flexibility. The effect of ramping rate on graphene foam flexibility was not conclusive. Therefore, in order to optimize the flexibility of graphene foam synthesized from this procedure, we may select an annealing temperature of 800°C, an annealing time of 15 minutes, and a ramping rate of 20°C/minute in order to maximize the flexibility of the sample while decreasing overall synthesis time.

Raman data suggests that as the annealing temperature is increased, the product purity increases, which correlates to an increase in thermal conductivity. However, when the annealing temperature is greater than 700°C, the increases in product purity become less significant. Therefore, it seems reasonable to use an annealing temperature of 800°C moving forward, as it allows for a relatively pure product while maintaining flexibility. Further investigation is needed in order to determine the effects of ramping rate and annealing time on product purity.

Qualitative assessment demonstrates that 13X zeolite yields the best packing of pores, compared to others tested. Therefore, this will be used moving forward with this project.

### **5.2 Future Work**

In the future, this project will be continued by others. Raman spectroscopy data will be collected as soon as equipment is available. This will provide accurate information about our samples in particular. This will provide a more accurate analysis of the characteristics of these particular samples. In addition, samples will be shipped for thermal conductivity testing. In doing

so, the synthesis procedure for graphene foam can be optimized in order to maximize thermal conductivity as well as flexibility.

In addition, mechanical strength testing can be improved by utilizing a hydraulic press rather than manual compression in order to assure that a uniform amount of pressure is applied to each graphene sample. Variation in pressure applied could result in inconsistent data.

Addition of zeolite to graphene foam will be studied on a more in-depth scale. Variables that may be considered include the use of different solvents to encourage the adsorption of zeolite into the pores of the graphene foam, and assessment of the amount of zeolite adsorbed. In addition, the stability of the zeolite-graphene foam composite when exposed to various conditions may be analyzed.

Given that the ultimate goal of this project is to develop a material that may be used in a water harvester, characterization of the zeolite-graphene composite's affinity for water is an important quality. Assessment of the material's compatibility with its intended function is important for the end goal of this project. Exposing samples to appropriate conditions, such as ambient temperature change and low relative humidity, the amount of water absorbed by the sample could be assessed by weighing the sample before and after leaving it to absorb water. This could be used as a proof of concept before scaling up the production of this material for use in a prototype device. Similar methods of testing were used in other works [2].

## References

1. Kummu, M., et al., *The world's road to water scarcity: shortage and stress in the 20th century and pathways towards sustainability*. Scientific reports, 2016. **6**: p. 38495-38495.
2. Kim, H., et al., *Water harvesting from air with metal-organic frameworks powered by natural sunlight*. Science, 2017. **356**(6336): p. 430.
3. Fathieh, F., et al., *Practical water production from desert air*. Science Advances, 2018. **4**(6): p. eaat3198.
4. Tu, Y., et al., *Progress and Expectation of Atmospheric Water Harvesting*. Joule, 2018. **2**(8): p. 1452-1475.
5. Rieth, A.J., et al., *Record Atmospheric Fresh Water Capture and Heat Transfer with a Material Operating at the Water Uptake Reversibility Limit*. ACS Central Science, 2017. **3**(6): p. 668-672.
6. Zhang, S., et al., *Bioinspired Special Wettability Surfaces: From Fundamental Research to Water Harvesting Applications*. Small, 2017. **13**(3): p. 1602992.
7. Kashiwa, B.A. and C.B. Kashiwa, *The solar cyclone: A solar chimney for harvesting atmospheric water*. Energy, 2008. **33**(2): p. 331-339.
8. Darryl Jones, G.C., *Solar Atmospheric Water Harvester*, U. States, Editor. 2008, Hydrotower Pty Limited: United States.
9. Max, M.D., *Apparatus and Method for Harvesting Atmospheric Moisture* , U.S.P. Office, Editor. 2005, Marine Desalination Systems, L.L.C.
10. James W. Hill, C.G.P., Micheal D. Max, *Atmospheric Water Harvesters*, U.S.P. Office, Editor. 2014, Water Generating Systems LLC.
11. Inagaki, M., J. Qiu, and Q. Guo, *Carbon foam: Preparation and application*. Carbon, 2015. **87**: p. 128-152.
12. Tjandra, R., et al., *Melamine based, n-doped carbon/reduced graphene oxide composite foam for Li-ion Hybrid Supercapacitors*. Carbon, 2018. **129**: p. 152-158.
13. Aleksandrak, M., W. Kukulka, and E. Mijowska, *Graphitic carbon nitride/graphene oxide/reduced graphene oxide nanocomposites for photoluminescence and photocatalysis*. Applied Surface Science, 2017. **398**: p. 56-62.
14. Chen, S., et al., *Elastic carbon foam via direct carbonization of polymer foam for flexible electrodes and organic chemical absorption*. Vol. 6. 2013.
15. Onwudili, J., et al., *High temperature pyrolysis of solid products obtained from rapid hydrothermal pre-processing of pinewood sawdust*. Vol. 4. 2014.
16. Sheng, Z.-H., et al., *Catalyst-Free Synthesis of Nitrogen-Doped Graphene via Thermal Annealing Graphite Oxide with Melamine and Its Excellent Electrocatalysis*. ACS Nano, 2011. **5**(6): p. 4350-4358.
17. Liu, W., et al., *Flexible and Stretchable Energy Storage: Recent Advances and Future Perspectives*. Advanced Materials, 2017. **29**(1): p. 1603436.
18. He, S. and W. Chen, *High performance supercapacitors based on three-dimensional ultralight flexible manganese oxide nanosheets/carbon foam composites*. Journal of Power Sources, 2014. **262**: p. 391-400.

19. Stolz, A., et al., *Melamine-derived carbon sponges for oil-water separation*. Carbon, 2016. **107**: p. 198-208.
20. Chen, B., et al., *Carbon-Based Sorbents with Three-Dimensional Architectures for Water Remediation*. Small, 2015. **11**(27): p. 3319-3336.
21. Ma, Q., et al., *Recent Development of Advanced Materials with Special Wettability for Selective Oil/Water Separation*. Small, 2016. **12**(16): p. 2186-2202.
22. Yang, S., et al., *Three-dimensional graphene enhanced heat conduction of porous crystals*. Journal of Porous Materials, 2016. **23**(6): p. 1647-1652.
23. Malard, L.M., et al., *Raman spectroscopy in graphene*. Physics Reports, 2009. **473**(5): p. 51-87.
24. Ferrari, A.C., *Raman spectroscopy of graphene and graphite: Disorder, electron-phonon coupling, doping and nonadiabatic effects*. Solid State Communications, 2007. **143**(1): p. 47-57.

## **Appendices**

### **Appendix 1: Safety Measures**

During this project, necessary safety measures were taken in order to assure that the lab remain a safe environment to conduct research. Closed toed shoes, protective eyewear, and gloves were worn at all time while working with chemicals. In addition, a single person was never left alone in the lab. All samples were properly labeled and stored so that they would not be disturbed by other students.

### **Appendix 2: Project Outcomes**

Preliminary results of this project were presented at the 2019 American Institute of Chemical Engineers Annual Meeting under the title of “Melamine-Derived Graphene Foam As a Thermal Additive.” In addition, this work was scheduled to be presented at the 2020 UTC Technology Symposium. However, due to the COVID-19 pandemic, this conference was canceled.

### **Appendix 3: Raw Data**

#### *Appendix 3.1: Flexibility Testing- Counts*

In this section, images used for counting the number of breaks per area are shown in Figure 27-Figure 54. Areas analyzed are inside of the rectangle on the image.

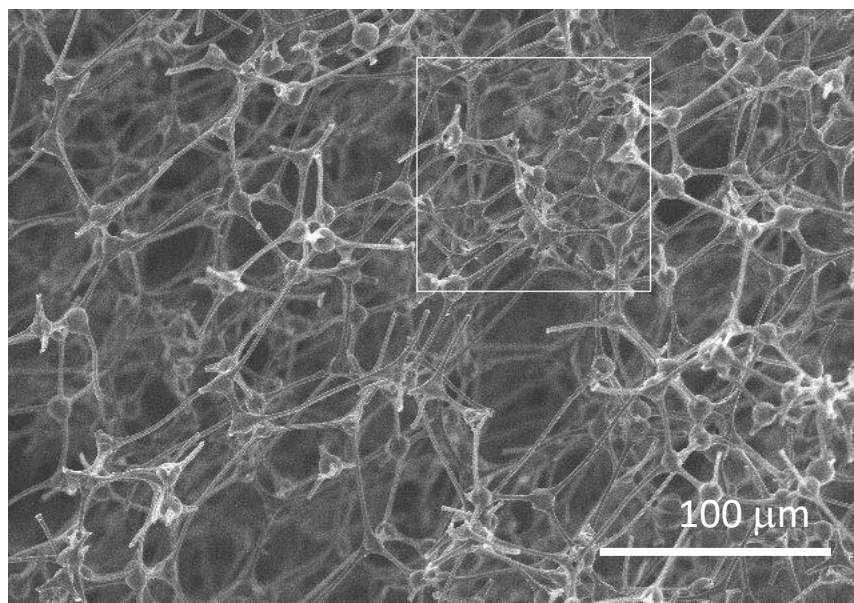


**Figure 27** SEM image 1 of graphene foam synthesized at 700°C, ramping rate of 10°C/min, and a total reaction time of 140 minutes (annealed for 70 minutes)

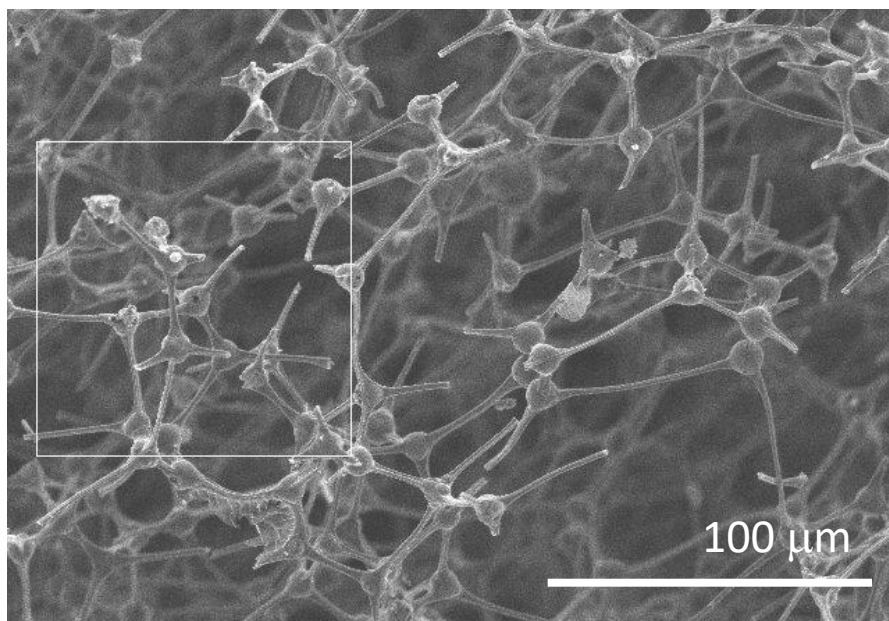


**Figure 28** SEM image 2 of graphene foam synthesized at 700°C, ramping rate of 10°C/min, and a total reaction time of 140 minutes (annealed for 70 minutes)

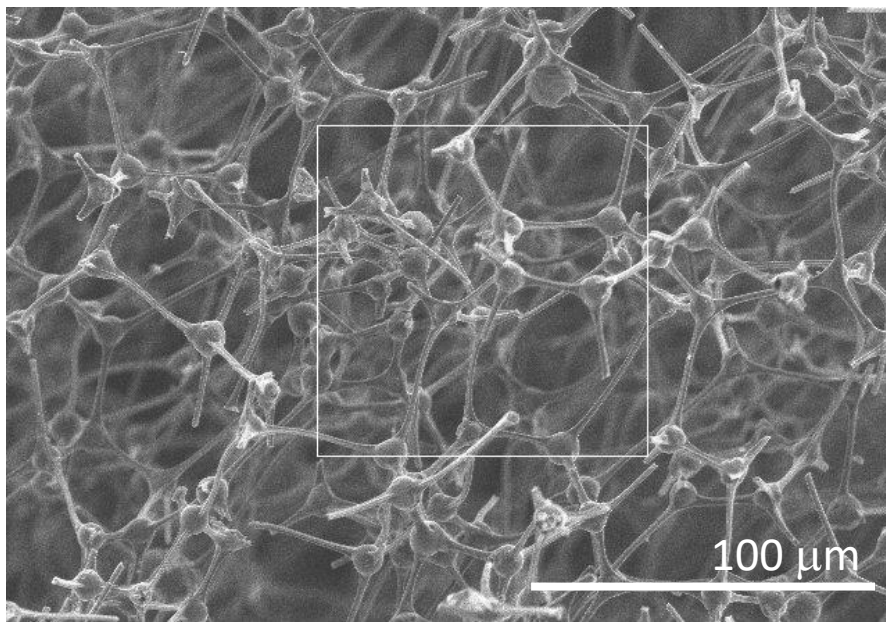


**Figure 29** SEM image 3 of graphene foam synthesized at 700°C, ramping rate of 10°C/min, and a total reaction time of 140 minutes (annealed for 70 minutes)

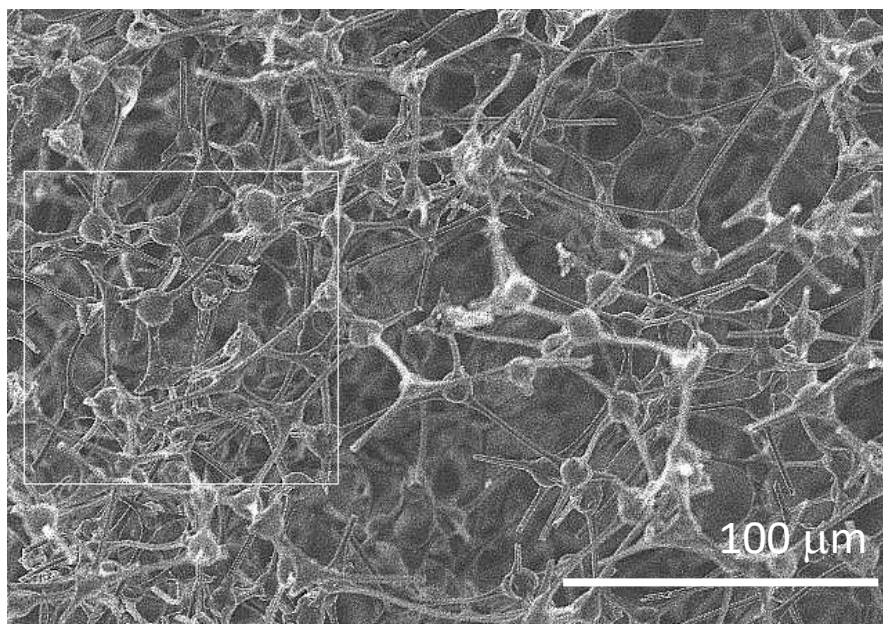


**Figure 30** SEM image 4 of graphene foam synthesized at 700°C, ramping rate of 10°C/min, and a total reaction time of 140 minutes (annealed for 70 minutes)

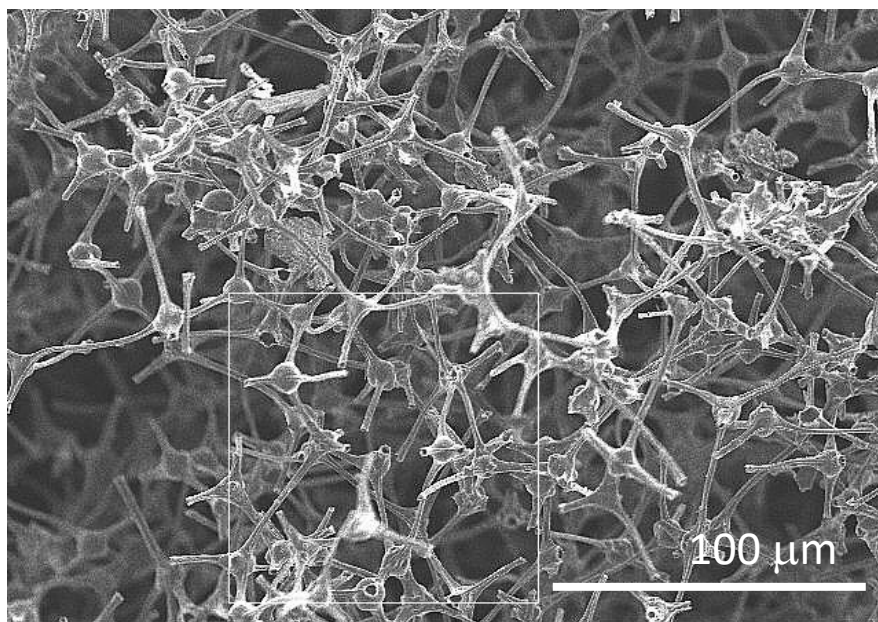


**Figure 31** SEM image 1 of graphene foam synthesized at 800°C, ramping rate of 10°C/min, and a total reaction time of 140 minutes (annealed for 60 minutes)

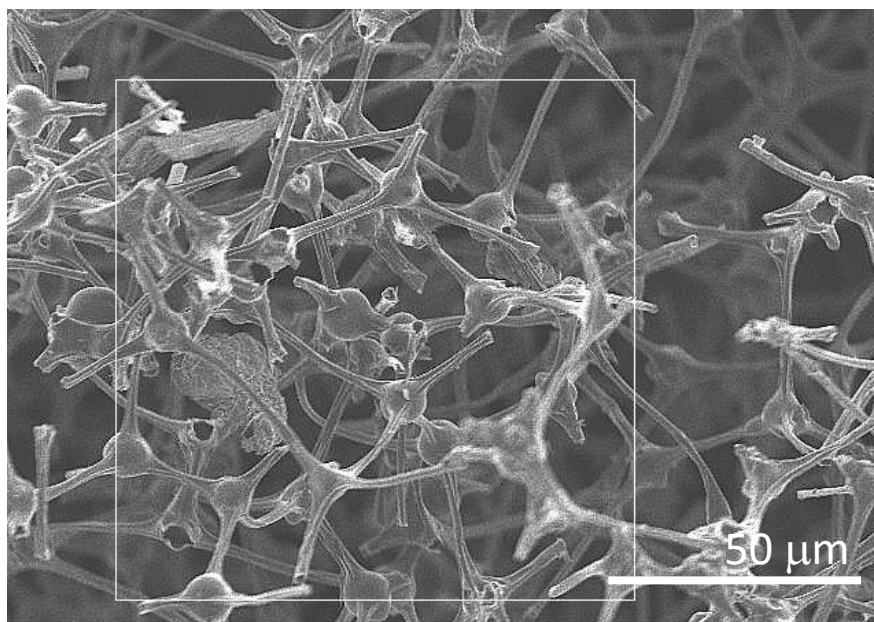


**Figure 32** SEM image 2 of graphene foam synthesized at 800°C, ramping rate of 10°C/min, and a total reaction time of 140 minutes (annealed for 60 minutes)

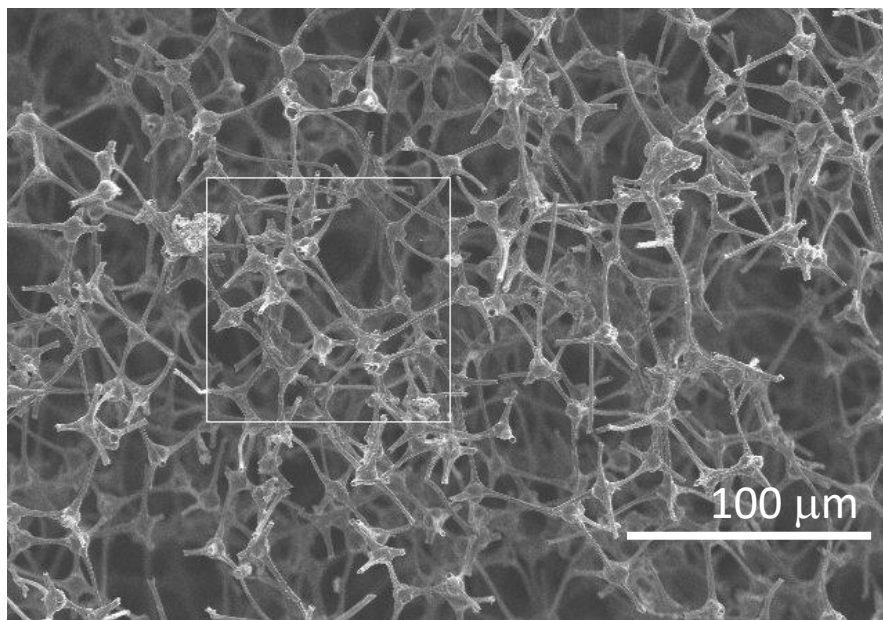


**Figure 33** SEM image 1 of graphene foam synthesized at 900°C, ramping rate of 10°C/min, and a total reaction time of 140 minutes (annealed for 50 minutes)

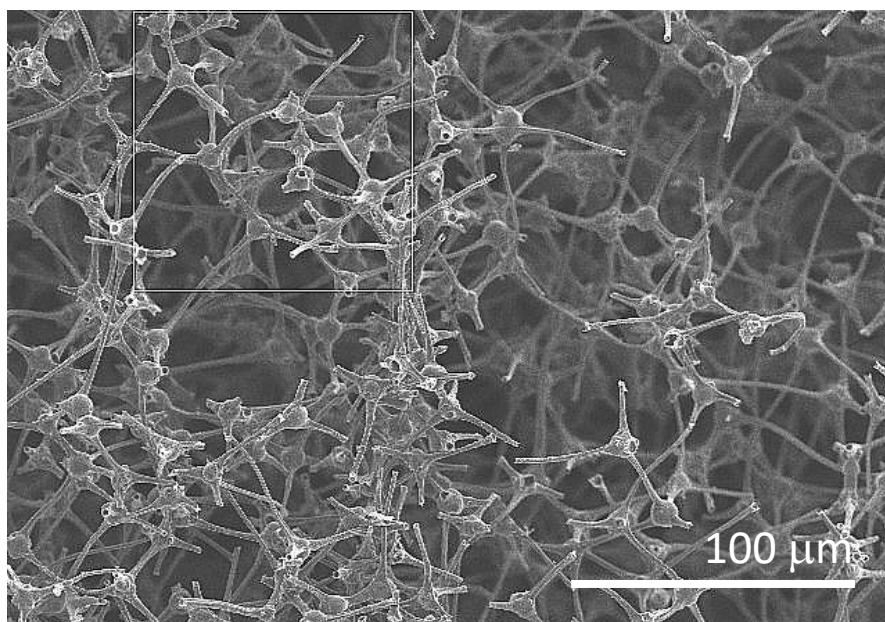


**Figure 34** SEM image 1 of graphene foam synthesized at 1000°C, ramping rate of 10°C/min, and a total reaction time of 140 minutes (annealed for 40 minutes)

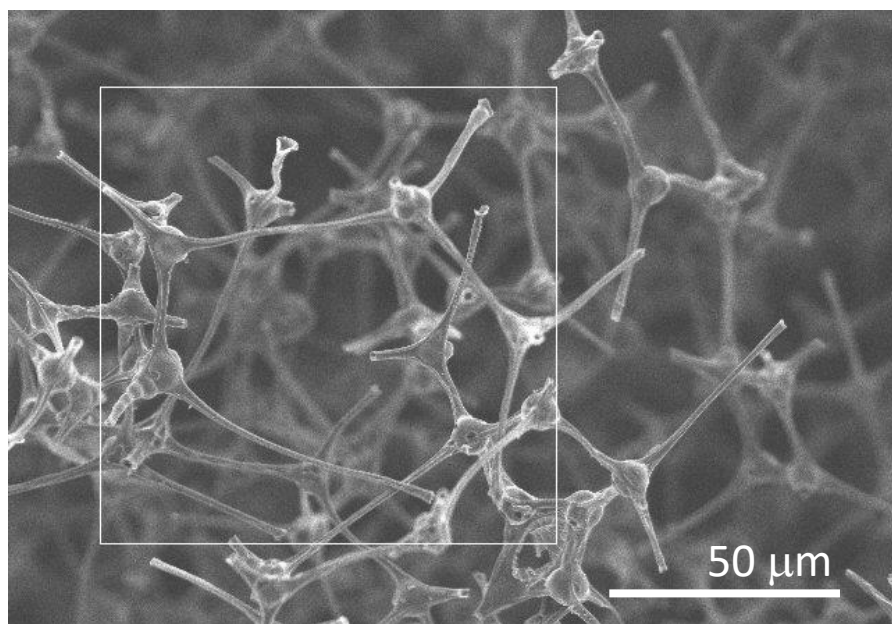


**Figure 35** SEM image 1 of graphene foam synthesized at 1000°C, ramping rate of 15°C/min, and a total reaction time of 140 minutes (annealed for 73 minutes)

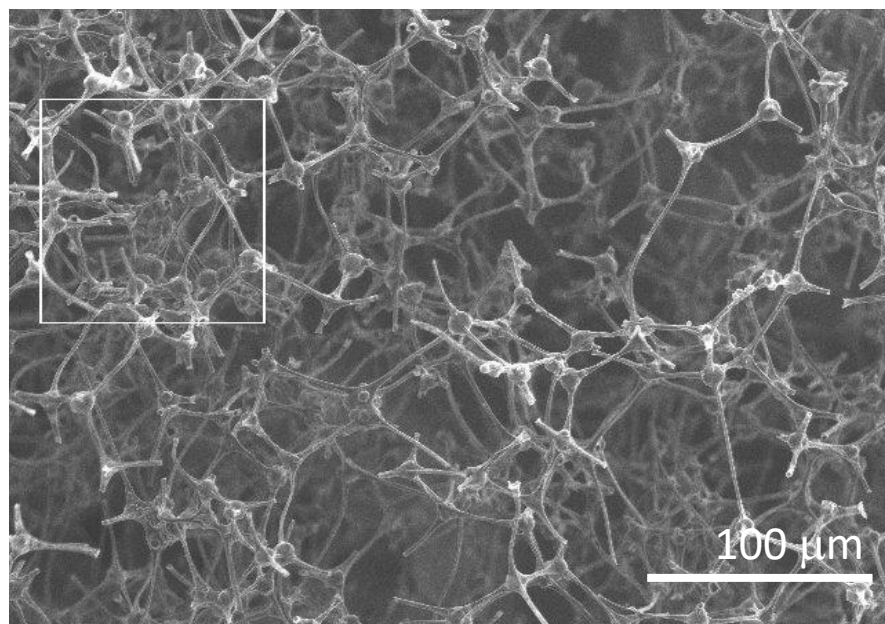


**Figure 36** SEM image 2 of graphene foam synthesized at 1000°C, ramping rate of 15°C/min, and a total reaction time of 140 minutes (annealed for 73 minutes)

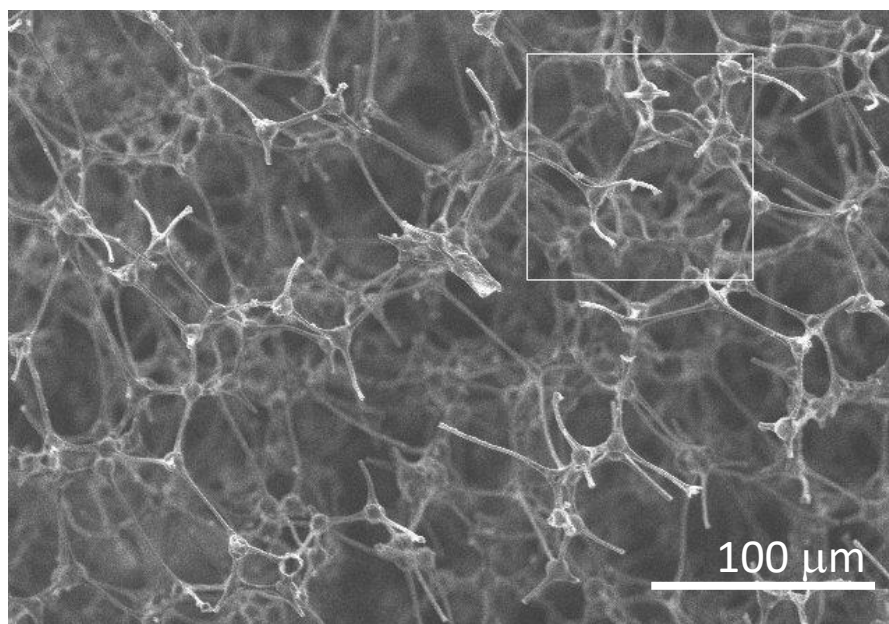


**Figure 37** SEM image 3 of graphene foam synthesized at 1000°C, ramping rate of 15°C/min, and a total reaction time of 140 minutes (annealed for 73 minutes)

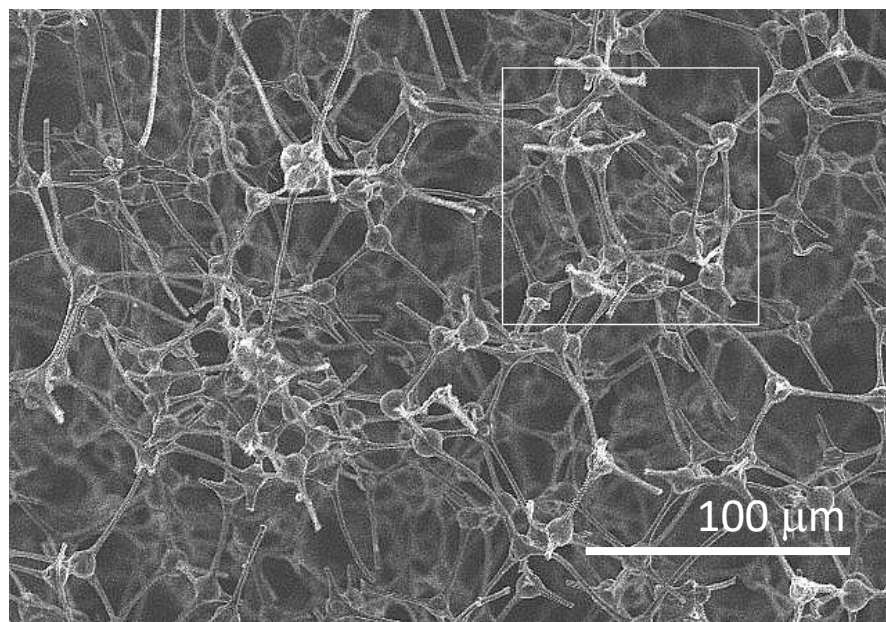


**Figure 38** SEM image 4 of graphene foam synthesized at 1000°C, ramping rate of 15°C/min, and a total reaction time of 140 minutes (annealed for 73 minutes)

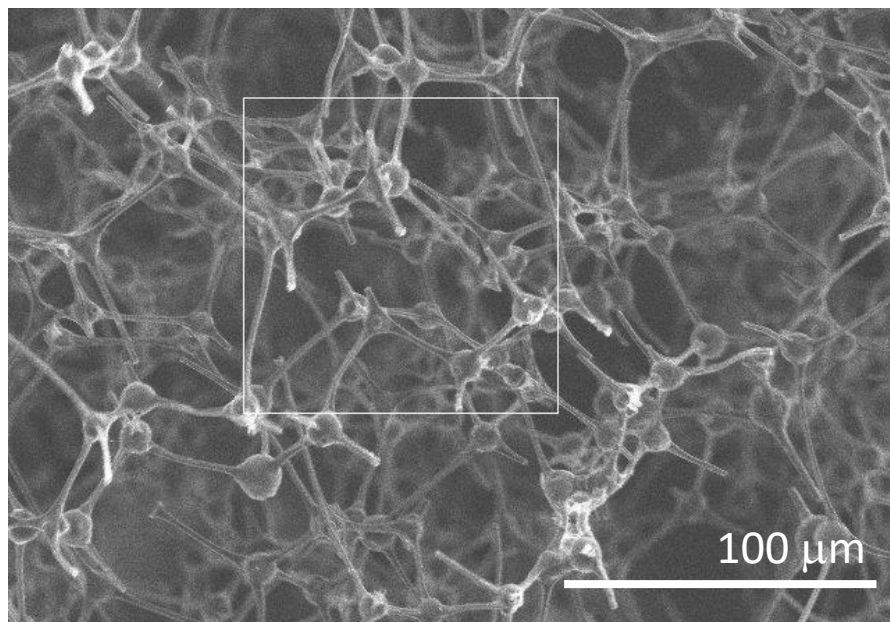


**Figure 39** SEM image 5 of graphene foam synthesized at 1000°C, ramping rate of 15°C/min, and a total reaction time of 140 minutes (annealed for 73 minutes)

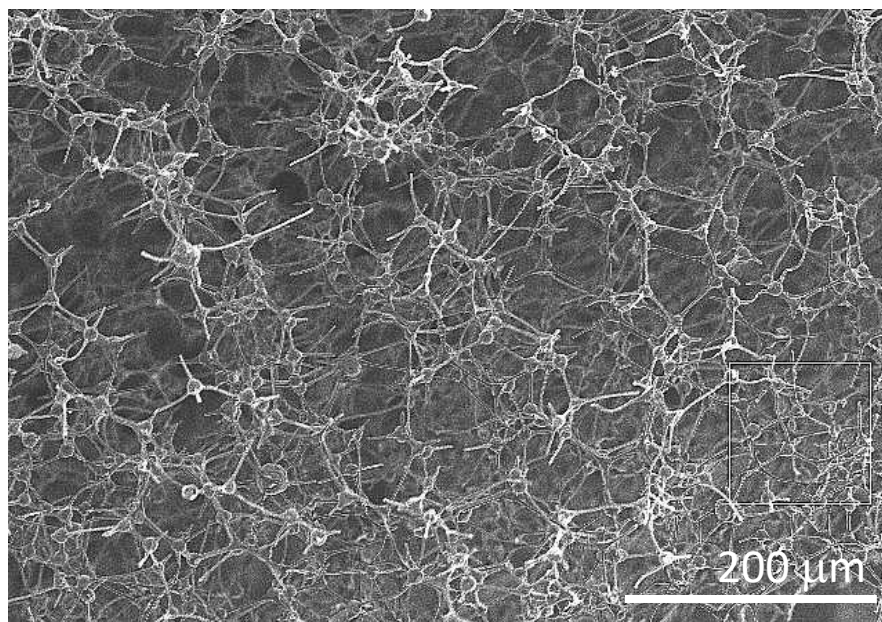


**Figure 40** SEM image 1 of graphene foam synthesized at 1000°C, ramping rate of 20°C/min, and a total reaction time of 140 minutes (annealed for 90 minutes)

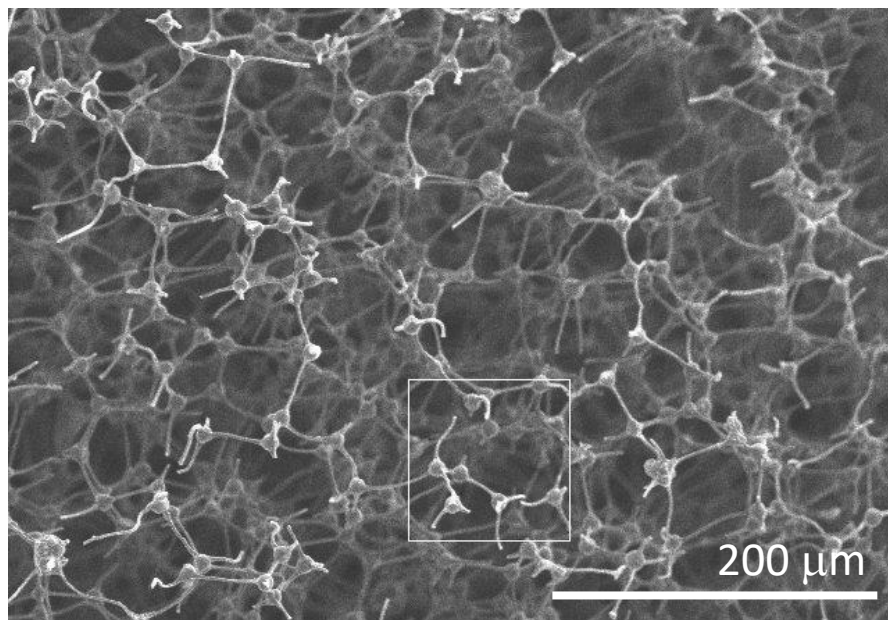


**Figure 41** SEM image 2 of graphene foam synthesized at 1000°C, ramping rate of 20°C/min, and a total reaction time of 140 minutes (annealed for 90 minutes)

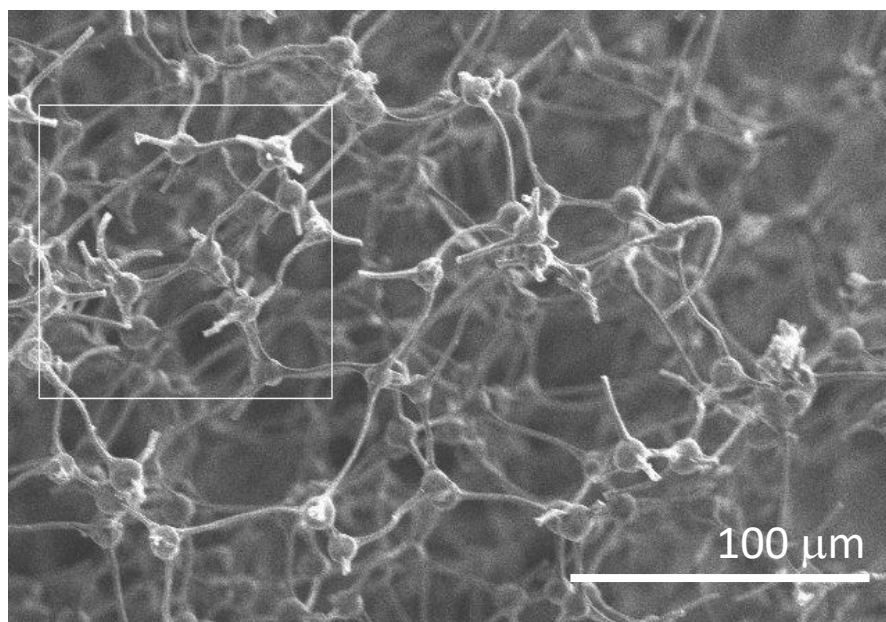


**Figure 42** SEM image 3 of graphene foam synthesized at 1000°C, ramping rate of 20°C/min, and a total reaction time of 140 minutes (annealed for 90 minutes)

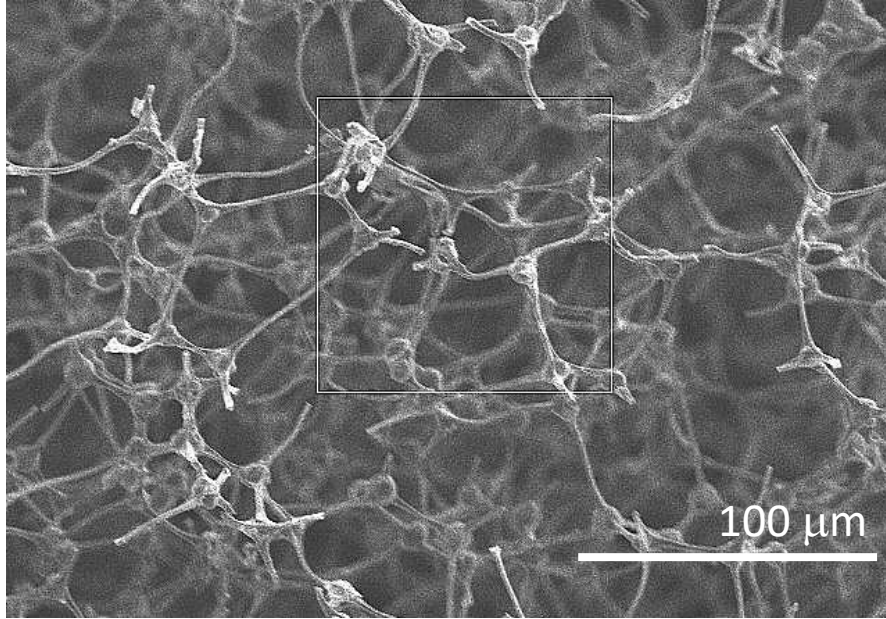


**Figure 43** SEM image 4 of graphene foam synthesized at 1000°C, ramping rate of 20°C/min, and a total reaction time of 140 minutes (annealed for 90 minutes)

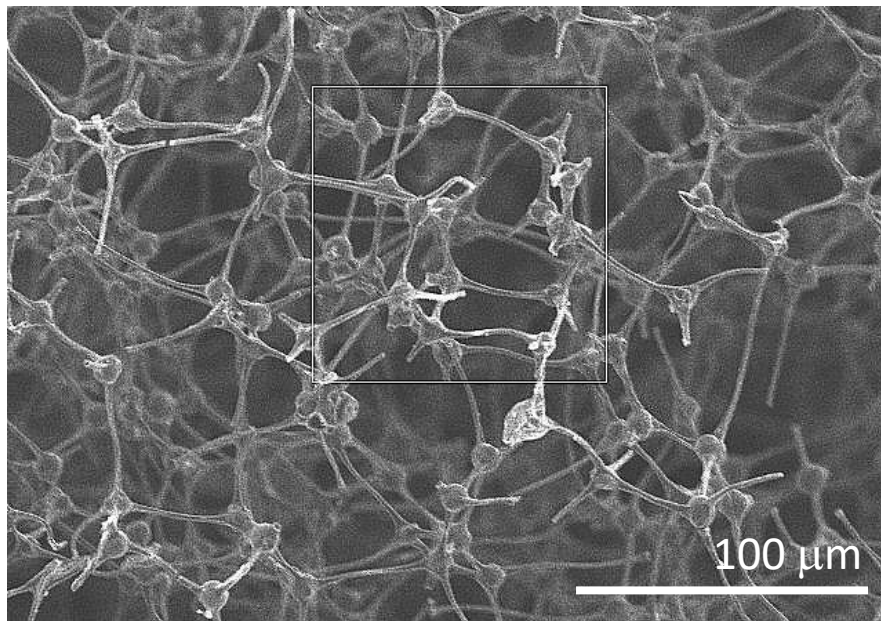


**Figure 44** SEM image 5 of graphene foam synthesized at 1000°C, ramping rate of 20°C/min, and a total reaction time of 140 minutes (annealed for 90 minutes)

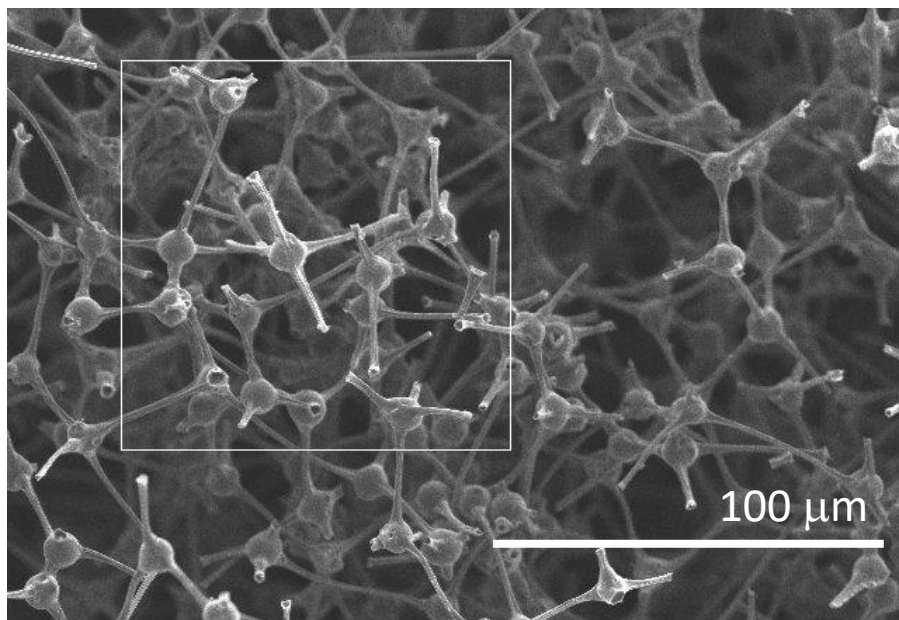


**Figure 45** SEM image 6 of graphene foam synthesized at 1000°C, ramping rate of 20°C/min, and a total reaction time of 140 minutes (annealed for 90 minutes)

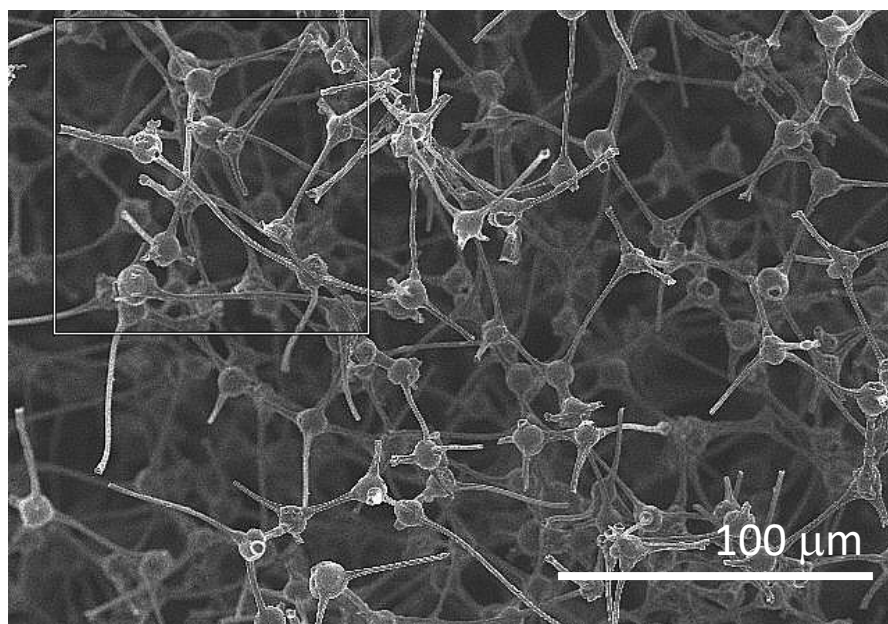


**Figure 46** SEM image 1 of graphene foam synthesized at 1000°C, ramping rate of 20°C/min, and a total reaction time of 65 minutes (annealed for 15 minutes)

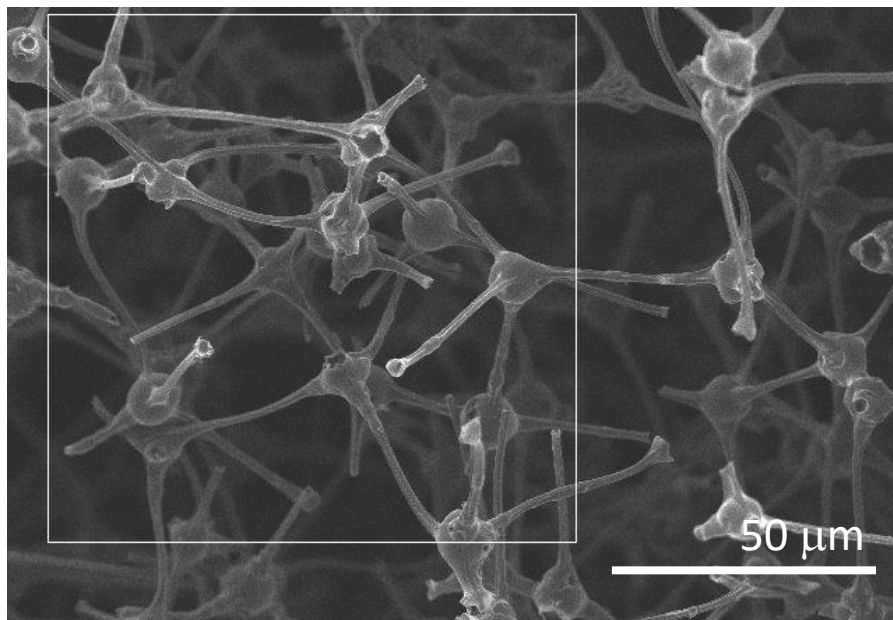


**Figure 47** SEM image 2 of graphene foam synthesized at 1000°C, ramping rate of 20°C/min, and a total reaction time of 65 minutes (annealed for 15 minutes)

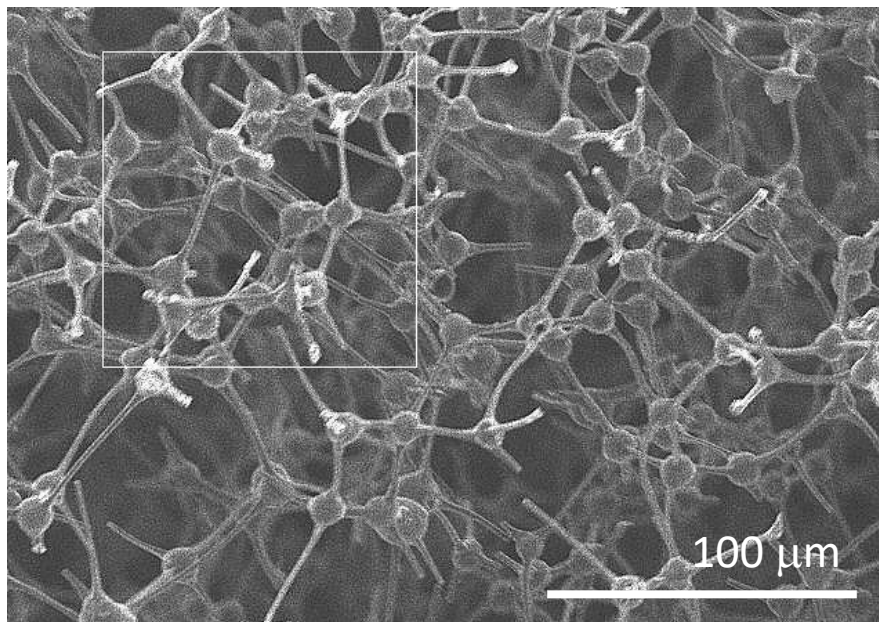


**Figure 48** SEM image 3 of graphene foam synthesized at 1000°C, ramping rate of 20°C/min, and a total reaction time of 65 minutes (annealed for 15 minutes)

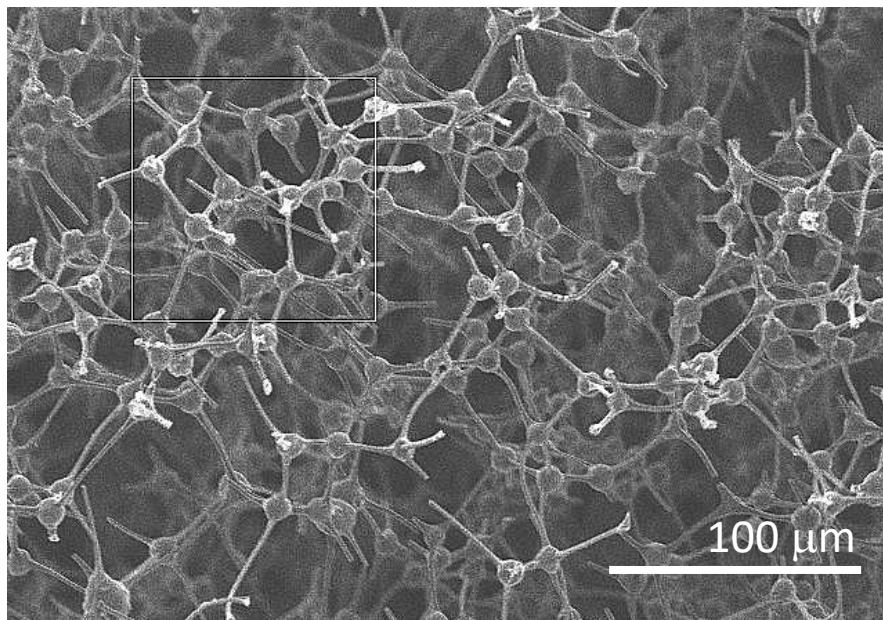


**Figure 49** SEM image 4 of graphene foam synthesized at 1000°C, ramping rate of 20°C/min, and a total reaction time of 65 minutes (annealed for 15 minutes)

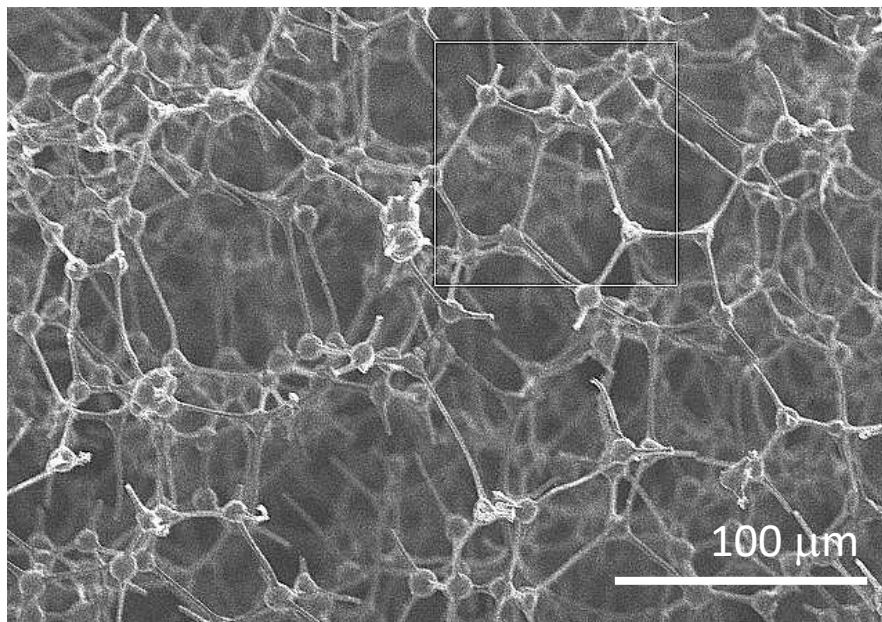


**Figure 50** SEM image 5 of graphene foam synthesized at 1000°C, ramping rate of 20°C/min, and a total reaction time of 65 minutes (annealed for 15 minutes)

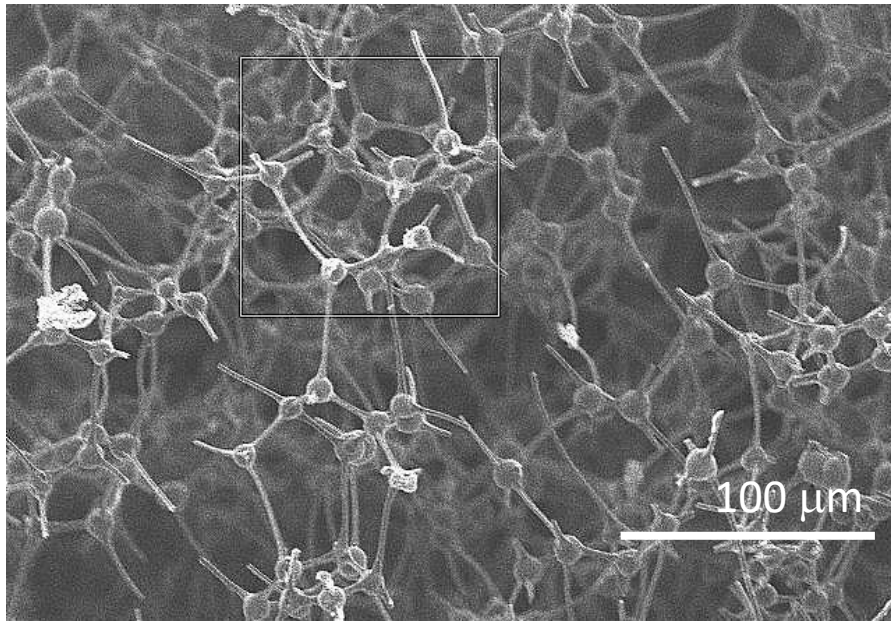


**Figure 51** SEM image 6 of graphene foam synthesized at 1000°C, ramping rate of 20°C/min, and a total reaction time of 65 minutes (annealed for 15 minutes)

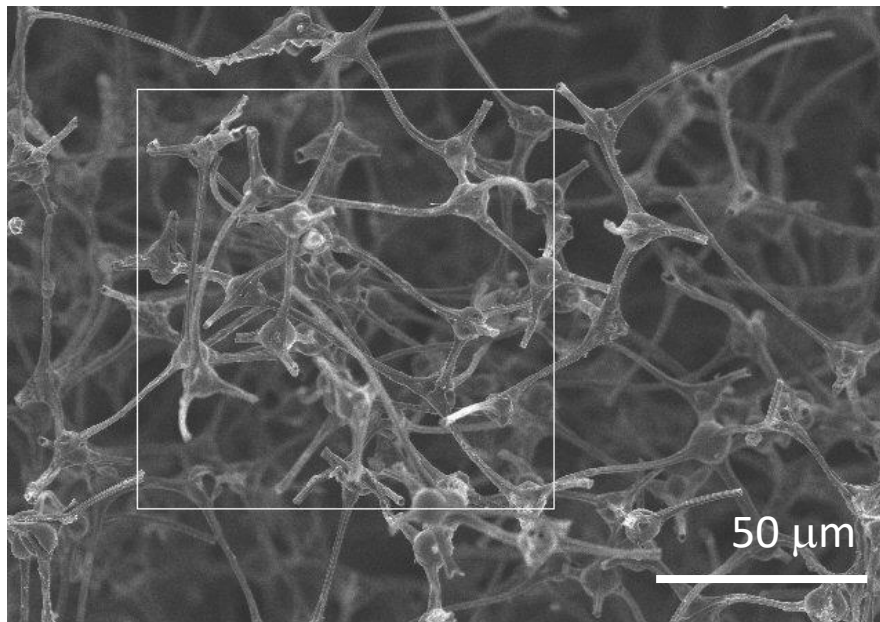


**Figure 52** SEM image 1 of graphene foam synthesized at 1000°C, ramping rate of 20°C/min, and a total reaction time of 80 minutes (annealed for 30 minutes)

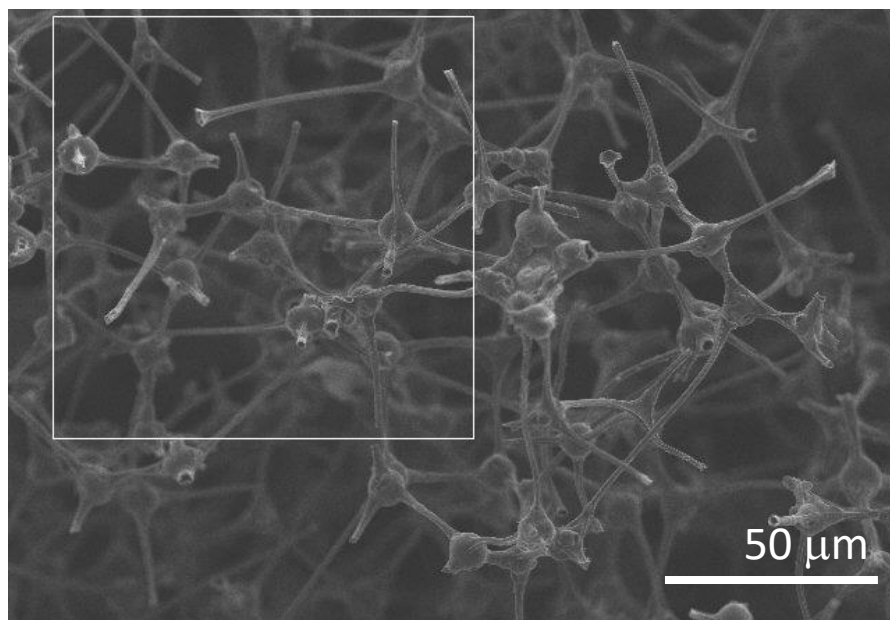


**Figure 53** SEM image 2 of graphene foam synthesized at 1000°C, ramping rate of 20°C/min, and a total reaction time of 80 minutes (annealed for 30 minutes)

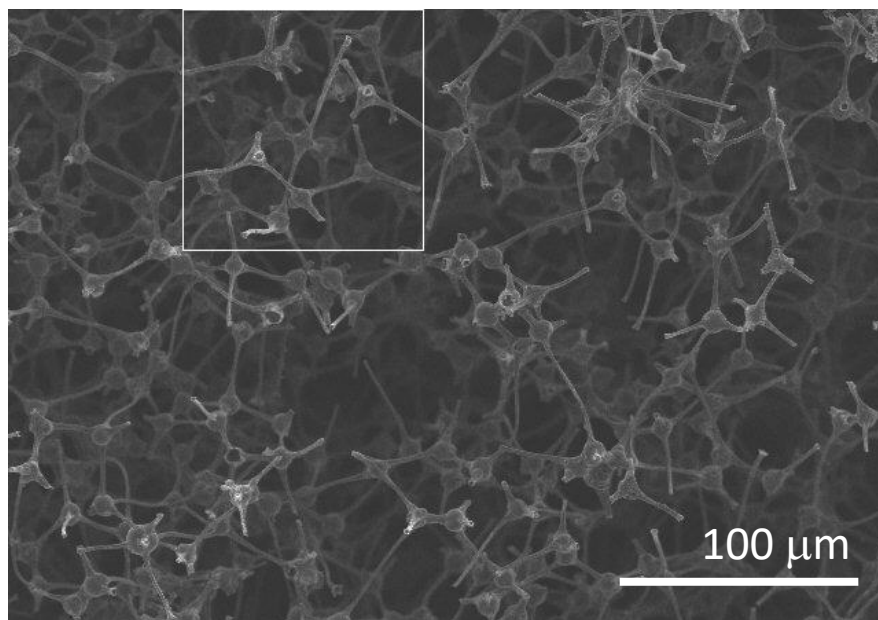


**Figure 54** SEM image 1 of graphene foam synthesized at 1000°C, ramping rate of 20°C/min, and a total reaction time of 95 minutes (annealed for 45 minutes)

*Appendix 3.2: Additional SEM Images*

Additional SEM images of individual strands of samples, which were qualitatively compared in section 4.1 are shown in Figure 55-Figure 73. These images provide more context to the claims made based on qualitative data.

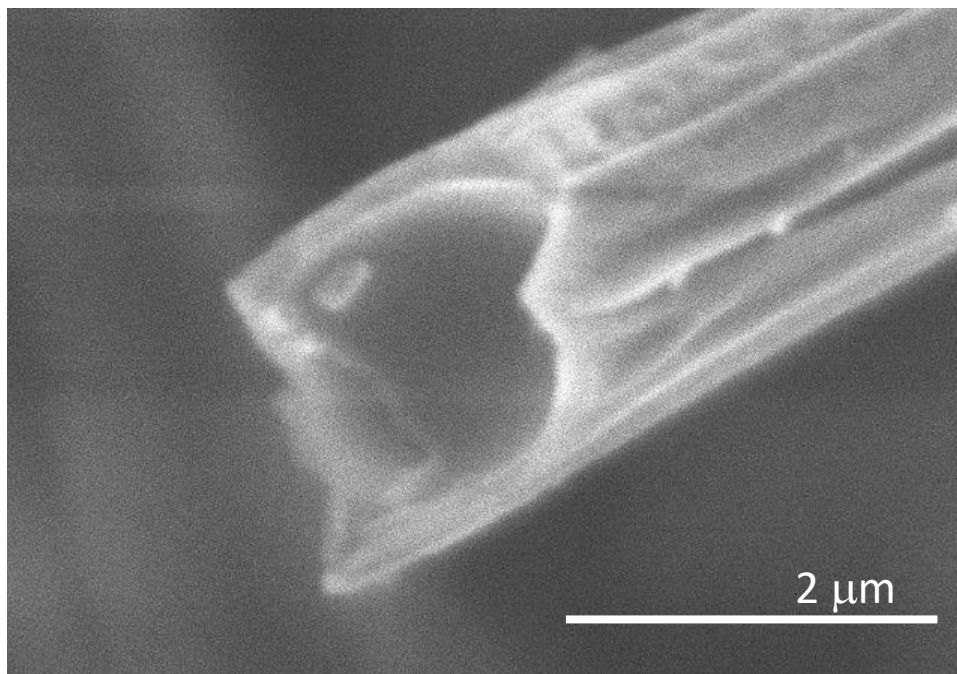


**Figure 55** Closeup image 1 of compressed graphene foam synthesized at 700°C, ramping rate of 10°C/min, and a total reaction time of 140 minutes (annealed for 70 minutes)

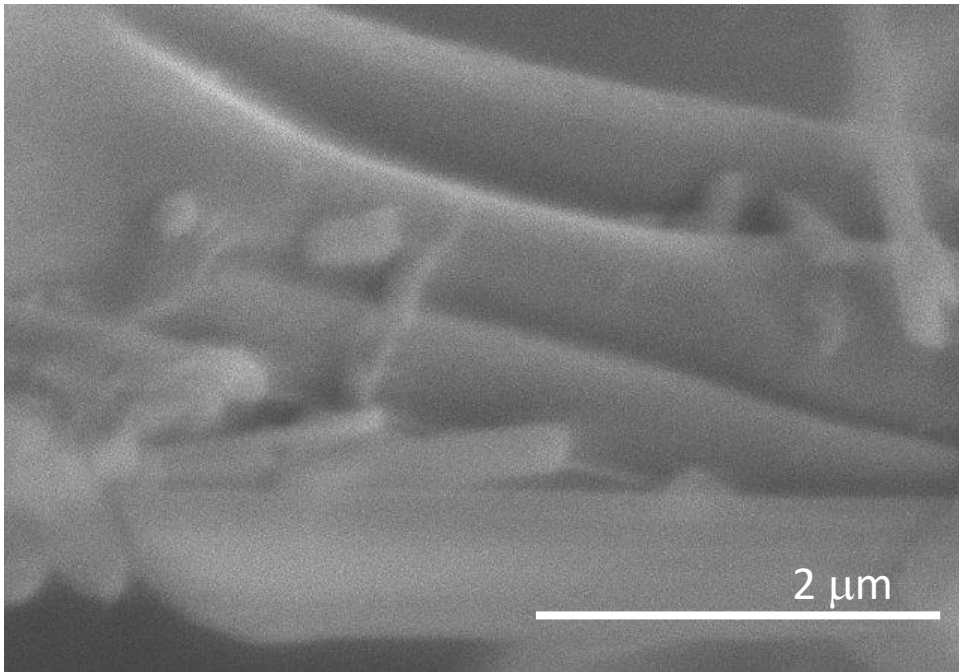


**Figure 56** Closeup image 2 of compressed graphene foam synthesized at 700°C, ramping rate of 10°C/min, and a total reaction time of 140 minutes (annealed for 70 minutes)

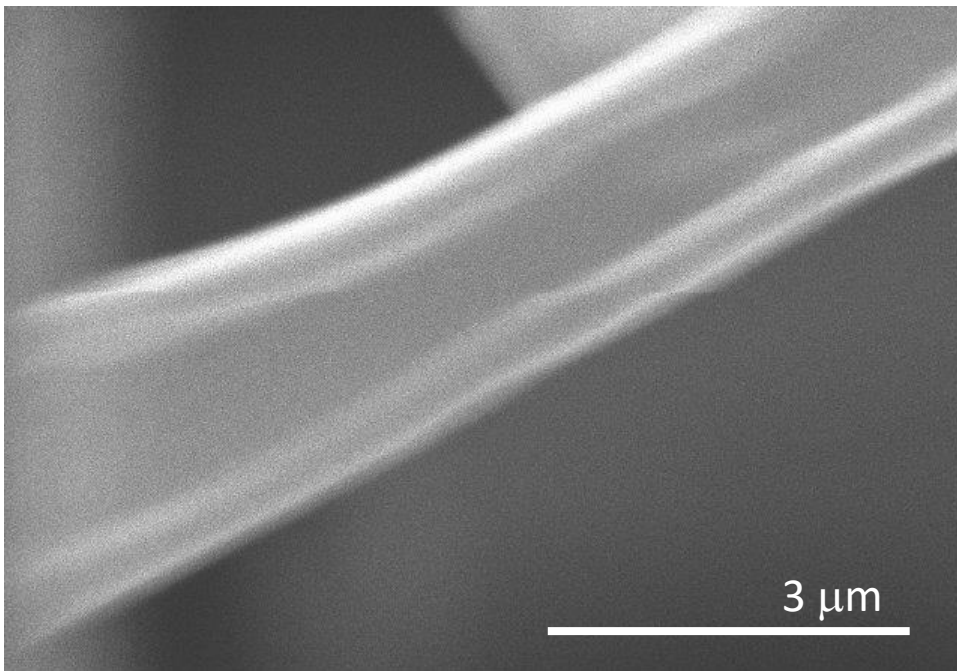


**Figure 57** Closeup image 1 of graphene foam synthesized at 800°C, ramping rate of 10°C/min, and a total reaction time of 140 minutes (annealed for 60 minutes)

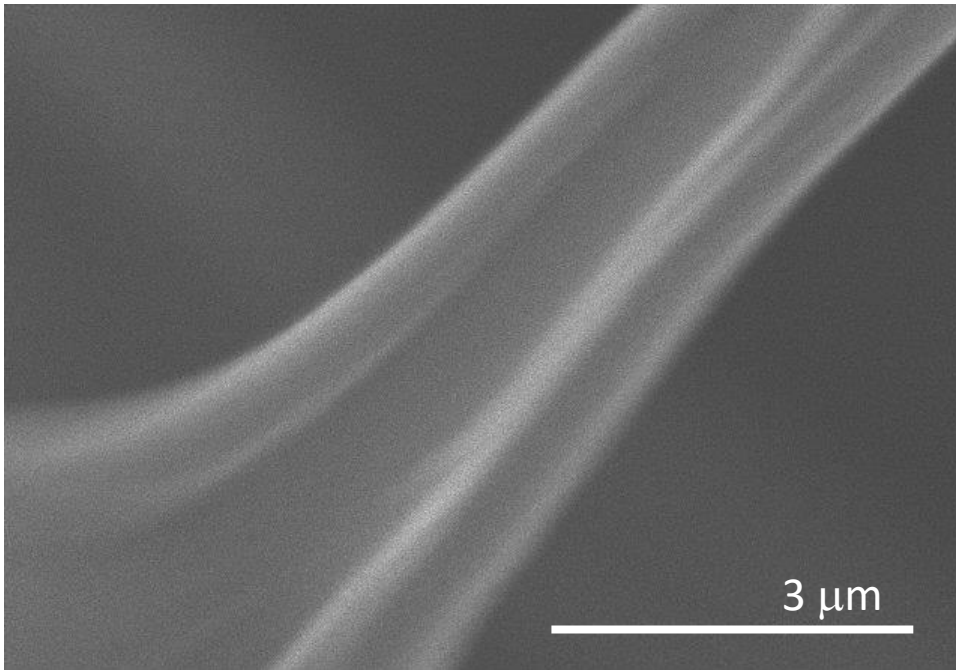


**Figure 58** Closeup image 1 of graphene foam synthesized at 900°C, ramping rate of 10°C/min, and a total reaction time of 140 minutes (annealed for 50 minutes)

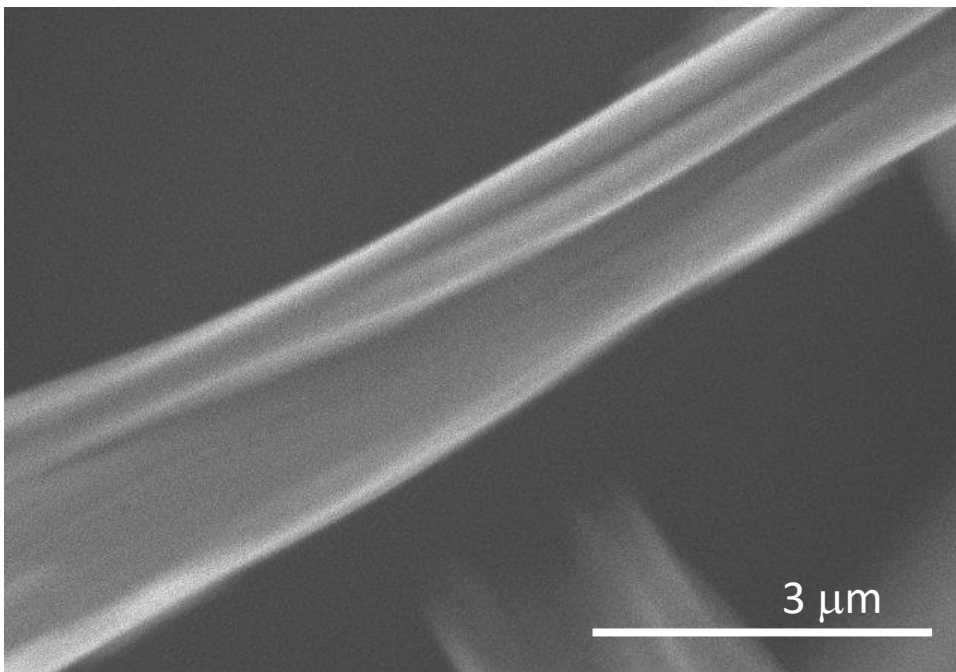


**Figure 59** Closeup image 2 of graphene foam synthesized at 900°C, ramping rate of 10°C/min, and a total reaction time of 140 minutes (annealed for 50 minutes)

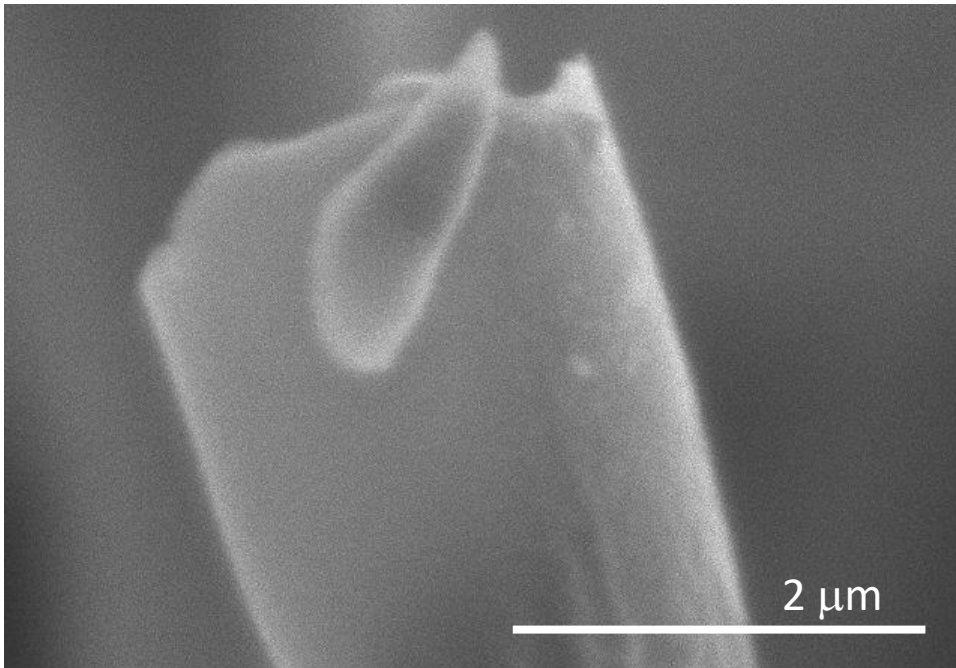


**Figure 60** Closeup image 1 of graphene foam synthesized at 1000°C, ramping rate of 10°C/min, and a total reaction time of 140 minutes (annealed for 40 minutes)

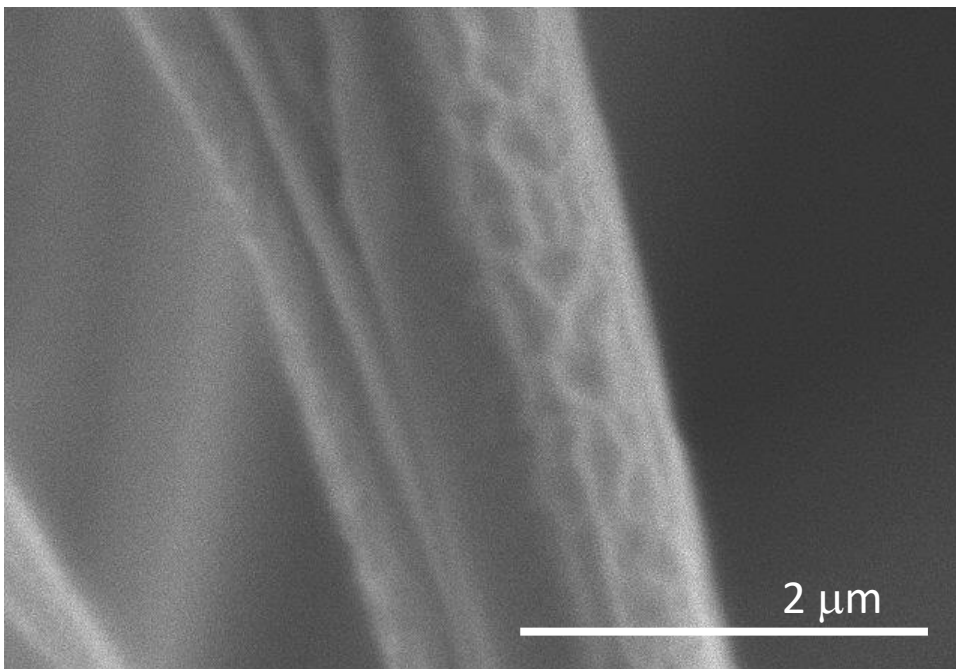


**Figure 61** Closeup image 2 of graphene foam synthesized at 1000°C, ramping rate of 10°C/min, and a total reaction time of 140 minutes (annealed for 40 minutes)

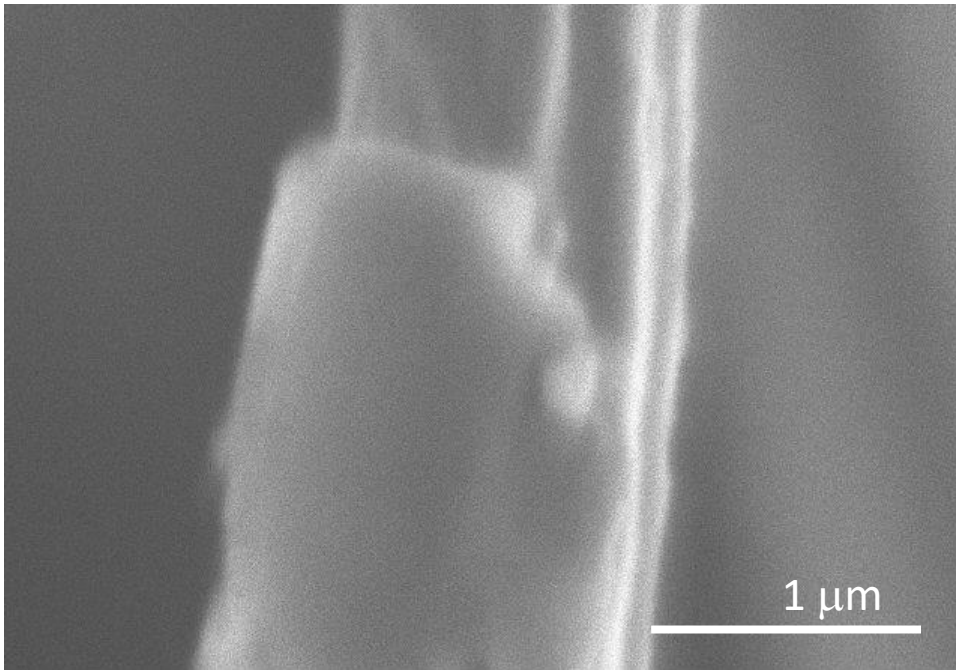


**Figure 62** Closeup image 3 of graphene foam synthesized at 1000°C, ramping rate of 10°C/min, and a total reaction time of 140 minutes (annealed for 40 minutes)

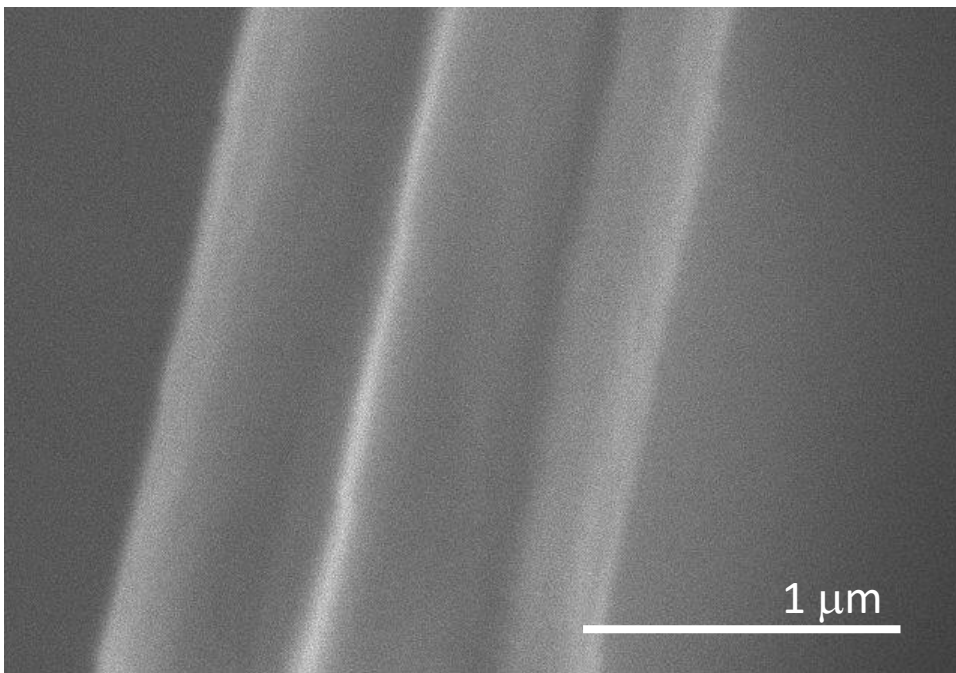


**Figure 63** Closeup image 4 of graphene foam synthesized at 1000°C, ramping rate of 10°C/min, and a total reaction time of 140 minutes (annealed for 40 minutes)

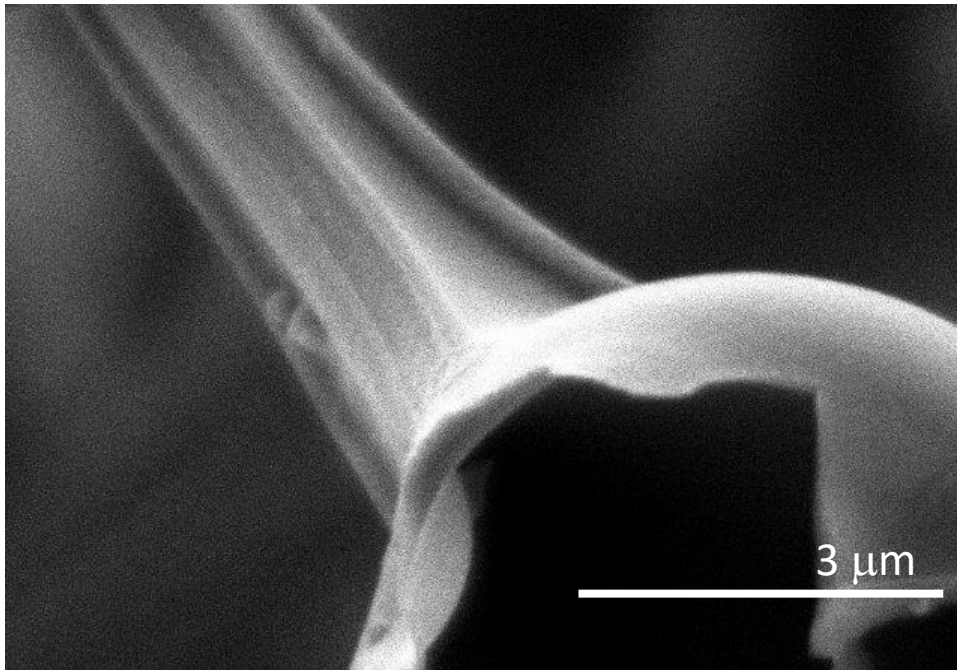


**Figure 64** Closeup image 1 of graphene foam synthesized at 1000°C, ramping rate of 15°C/min, and a total reaction time of 140 minutes (annealed for 73 minutes)

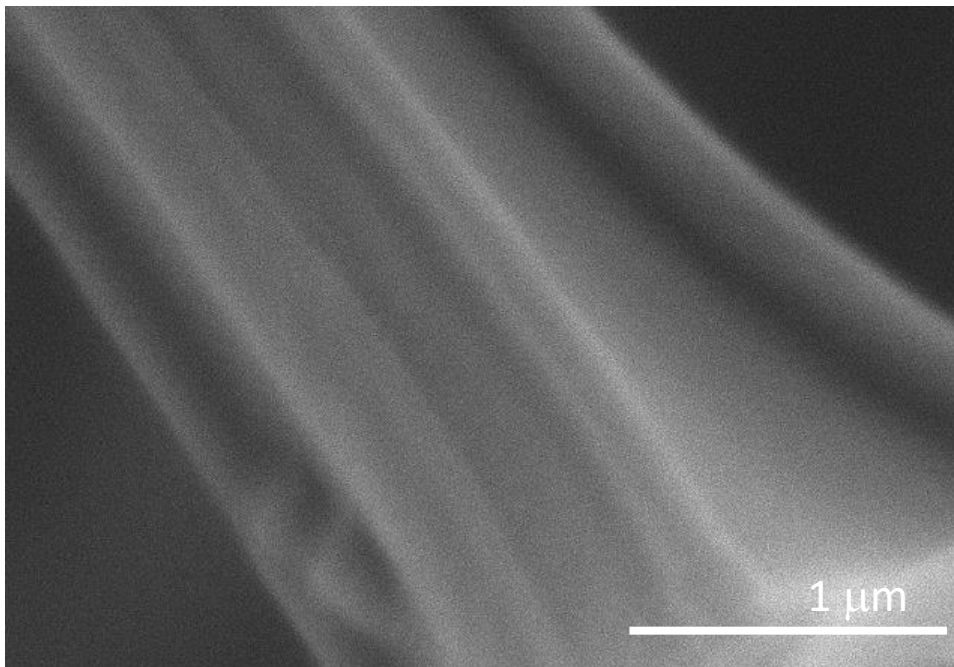


**Figure 65** Closeup image 2 of graphene foam synthesized at 1000°C, ramping rate of 15°C/min, and a total reaction time of 140 minutes (annealed for 73 minutes)

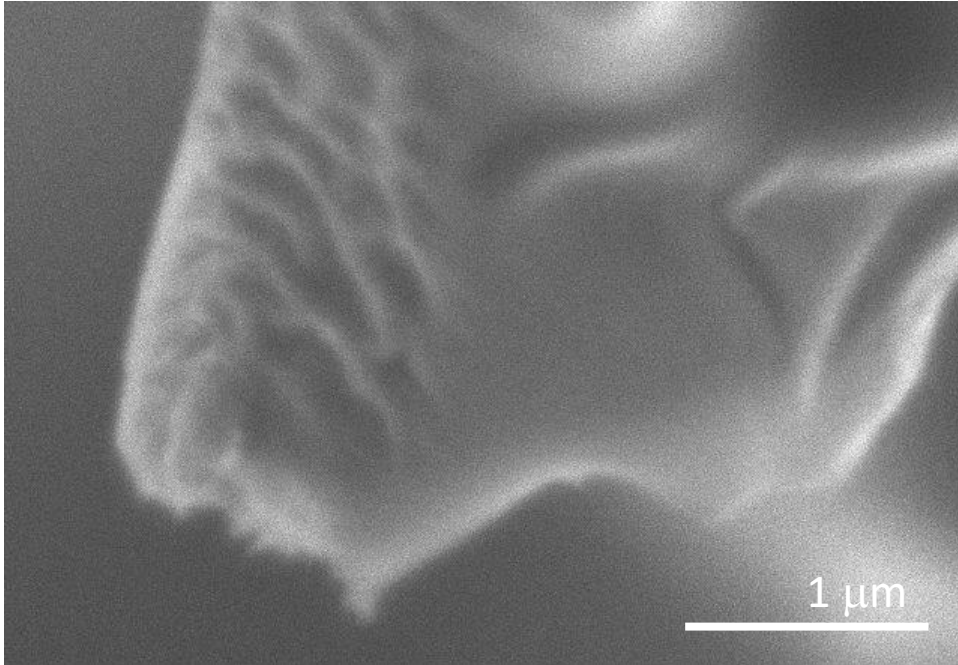


**Figure 66** Closeup image 1 of graphene foam synthesized at 1000°C, ramping rate of 20°C/min, and a total reaction time of 140 minutes (annealed for 90 minutes)

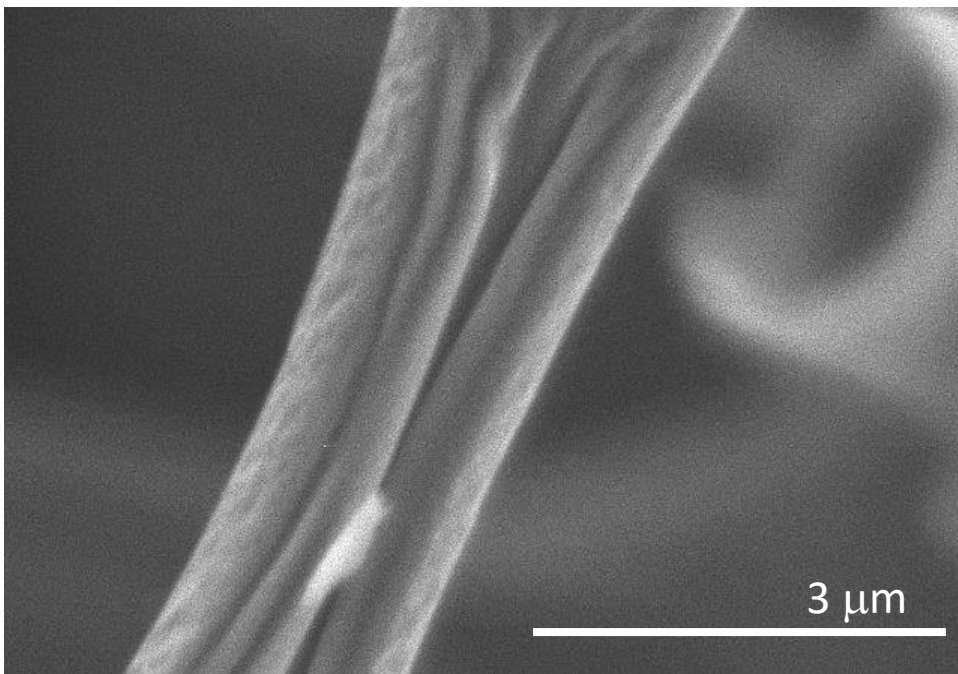


**Figure 67** Closeup image 2 of graphene foam synthesized at 1000°C, ramping rate of 20°C/min, and a total reaction time of 140 minutes (annealed for 90 minutes)

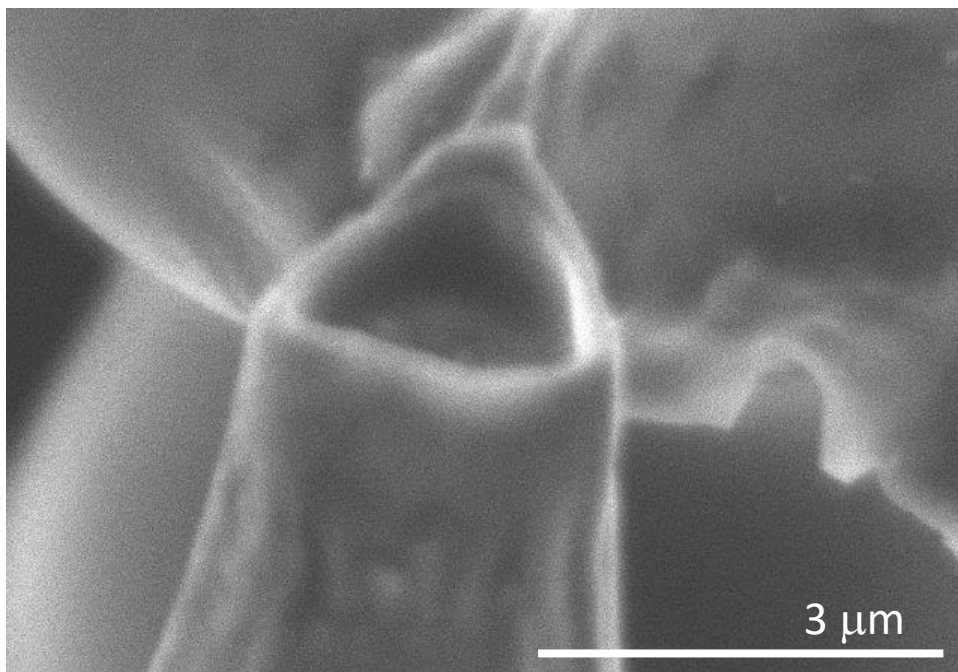


**Figure 68** Closeup image 1 of graphene foam synthesized at 1000°C, ramping rate of 20°C/min, and a total reaction time of 65 minutes (annealed for 15 minutes)

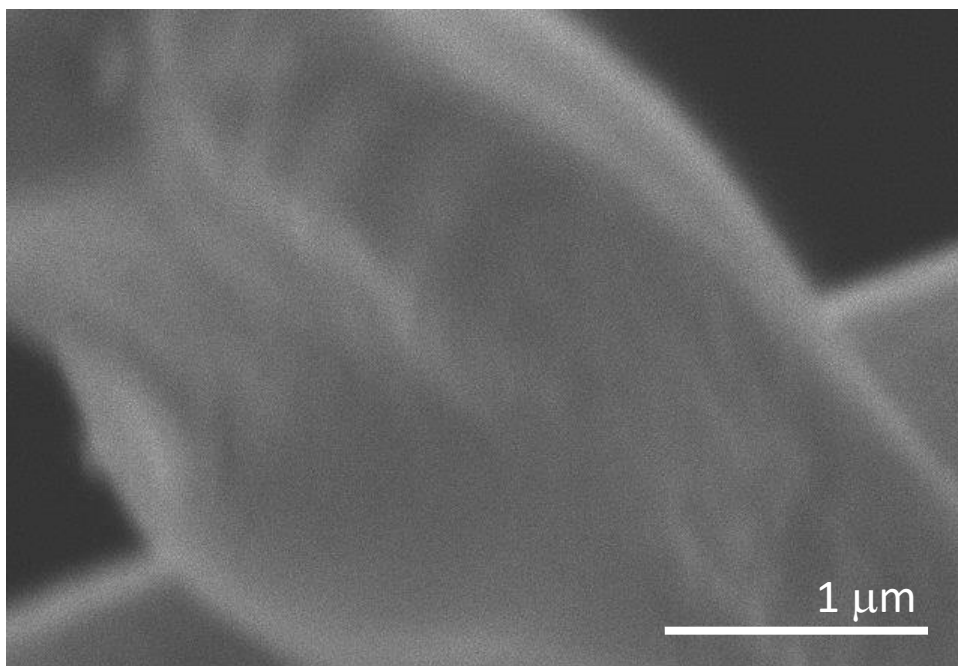


**Figure 69** Closeup image 2 of graphene foam synthesized at 1000°C, ramping rate of 20°C/min, and a total reaction time of 65 minutes (annealed for 15 minutes)

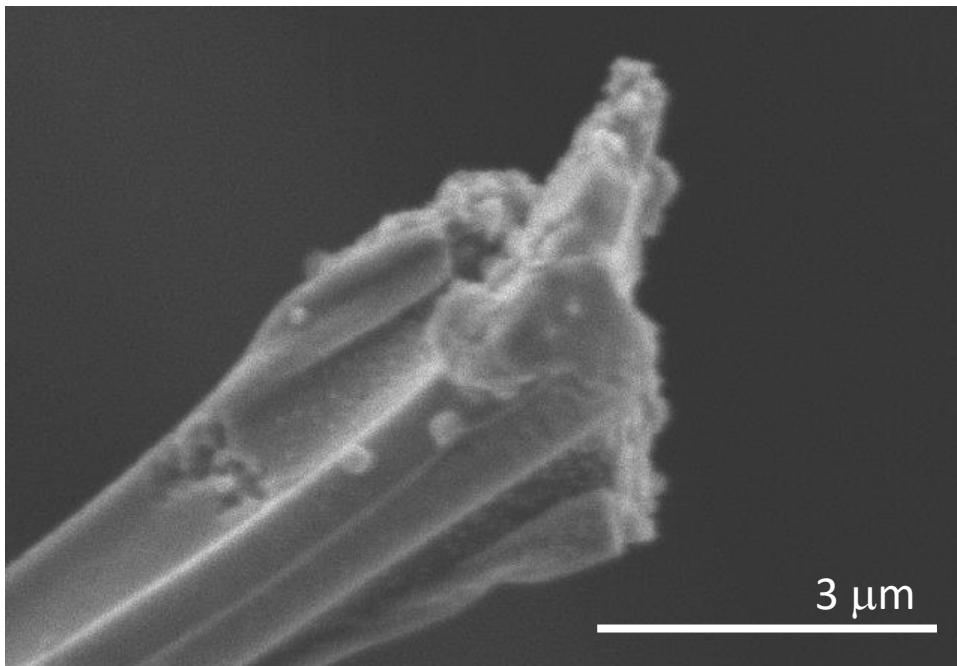


**Figure 70** Closeup image 1 of graphene foam synthesized at 1000°C, ramping rate of 20°C/min, and a total reaction time of 80 minutes (annealed for 30 minutes)

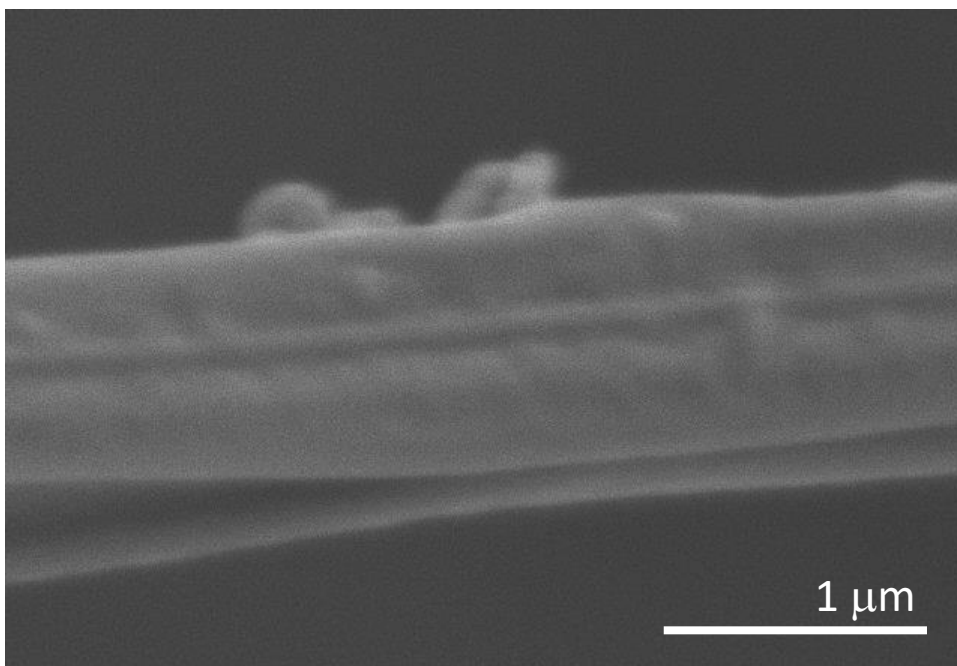


**Figure 71** Closeup image 2 of graphene foam synthesized at 1000°C, ramping rate of 20°C/min, and a total reaction time of 80 minutes (annealed for 30 minutes)

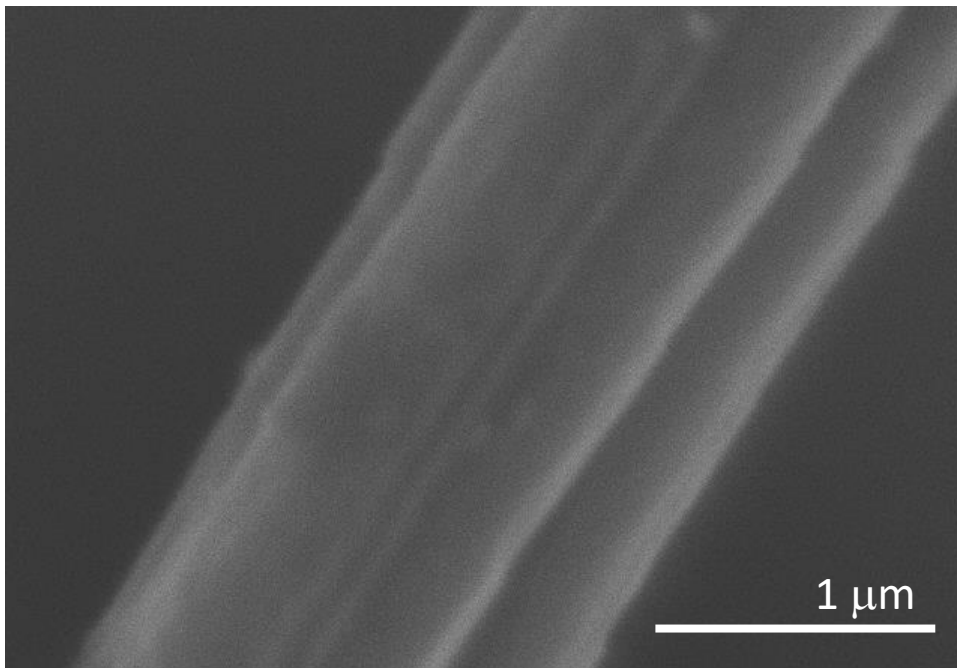


**Figure 72** Closeup image 1 of graphene foam synthesized at 1000°C, ramping rate of 20°C/min, and a total reaction time of 95 minutes (annealed for 45 minutes)

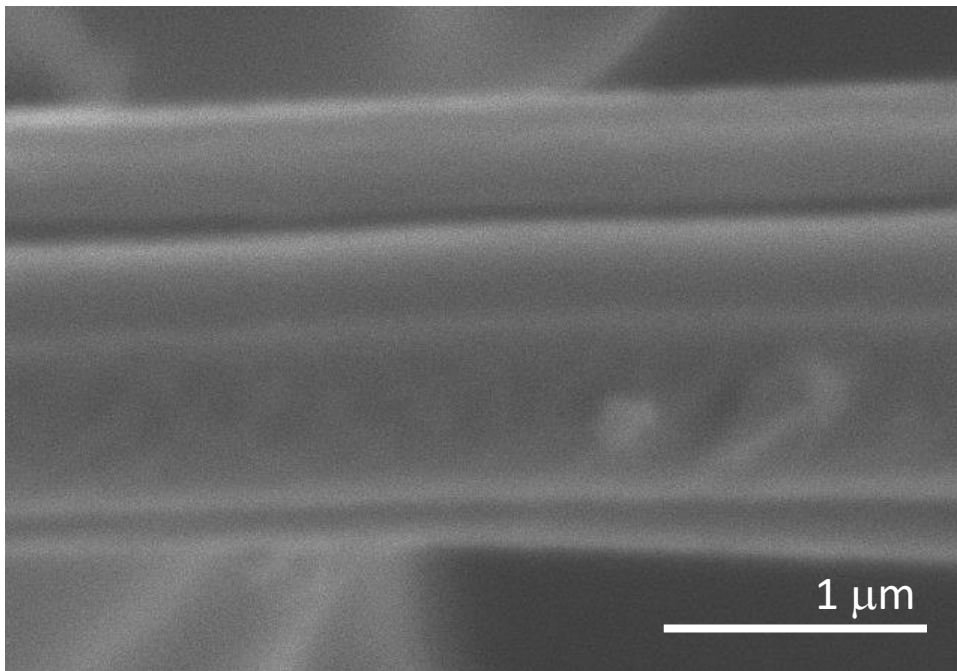


**Figure 73** Closeup image 2 of graphene foam synthesized at 1000°C, ramping rate of 20°C/min, and a total reaction time of 95 minutes (annealed for 45 minutes)